Energy, Mines and Resources Canada | Énergie, Mines et Ressources Canada

CANMET

Canada Centre for Mineral and Energy Technology | Centre canadien de la technologie des minéraux et de l'énergie

SPECIAL AMBIENT TEMPERATURE MECHANICAL PROPERTIES STUDIES TO DETERMINE THE EFFECTS OF STRESS RELEASE ON URL CORE SAMPLES

R. Jackson and C. Boudreau
Rock Mechanics Laboratory

MARCH 1984

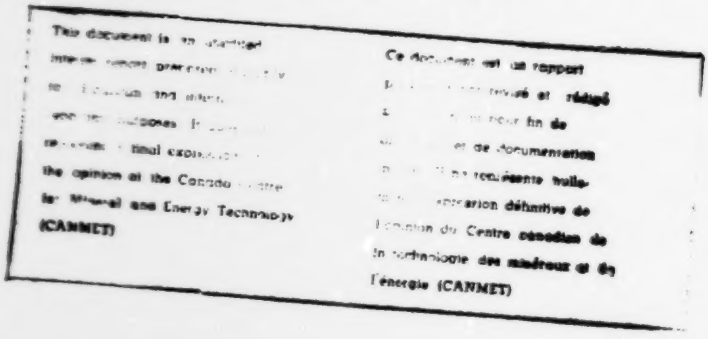

62 pp

ENERGY RESEARCH PROGRAM
MINING RESEARCH LABORATORIES
DIVISION REPORT ERP/MRL 84-17(TR)

OCT 26 1984
MICROMEDIA

85-0250/

CONTENTS

	Page
INTRODUCTION	1
IDENTIFICATION OF SPECIMENS AND TESTS	2
DESCRIPTION OF TEST MEASUREMENTS	2
DATA SUMMARY	3
BASIC DATA	4
SUMMARY AND CONCLUSIONS	4
REFERENCES	5

TABLES

No.		
1.	Borehole/horizon identification and major principle stresses	1
2.	Dimensions and density of specimens	3
3.	Summary of uniaxial compressive strength, zero pressure velocity and deformation property data of specimens	6
4.	Confined velocity measurements	7
5.	Brazilian tensile test results	12
6.	Results of triaxial tests on URL specimens	13

FIGURES

	Page
1. Tangent modulus of elasticity vs confining pressure: boreholes URL-2, 5 & 6	17
2. Axial and circumferential stress strain curves for URL-2 1080.32	18
3. Axial and circumferential stress strain curves for URL-2 1080.55	19

Figures (Cont'd)

No.		Page
4.	Axial and circumferential stress strain curves for URL-2 1080.83	20
5.	Axial and circumferential stress strain curves for URL-2 1081.06	21
6.	Axial and circumferential stress strain curves for URL-2 1081.67	22
7.	Axial and circumferential stress strain curves for URL-2 1081.90	23
8.	Axial and circumferential stress strain curves for URL-2 1082.21	24
9.	Axial and circumferential stress strain curves for URL-2 1082.44	25
10.	Axial and circumferential stress strain curves for URL-5 441.75	26
11.	Axial and circumferential stress strain curves for URL-5 441.98	27
12.	Axial and circumferential stress strain curves for URL-5 442.26	28
13.	Axial and circumferential stress strain curves for URL-5 442.54	29
14.	Axial and circumferential stress strain curves for URL-6 373.80	30
15.	Axial and circumferential stress strain curves for URL-6 374.70	31
16.	Axial and circumferential stress strain curves for URL-6 374.98	32
17.	Axial and circumferential stress strain curves for URL-6 391.38	33
18.	Axial and circumferential stress strain curves for URL-6 391.61	34

Figures (Cont'd) Page

No.

19. Axial and circumferential stress strain curves for URL-6 391.89 35
20. Axial and circumferential stress strain curves for URL-6 392.17 36
21. Deviatorial stress vs strain: URL-2 1080.14 (10 MPa) 37
22. Deviatorial stress vs strain: URL-2 1081.77 (10 MPa) 38
23. Deviatorial stress vs strain: URL-2 1080.41 (35 MPa) 39
24. Deviatorial stress vs strain: URL-2 1081.49 (35 MPa) 40
25. Deviatorial stress vs strain: URL-2 1080.93 (50 MPa) 41
26. Deviatorial stress vs strain: URL-2 1082.31 (50 MPa) 42
27. Deviatorial stress vs strain: URL-2 1080.63 (70 MPa) 43
28. Deviatorial stress vs strain: URL-2 1082.03 (70 MPa) 44
29. Deviatorial stress vs strain: URL-5 442.13 (15 MPa) 45
30. Deviatorial stress vs strain: URL-5 442.94 (15 MPa) 46
31. Deviatorial stress vs strain: URL-5 441.85 (30 MPa) 47
32. Deviatorial stress vs strain: URL-5 442.64 (30 MPa) 48
33. Deviatorial stress vs strain: URL-5 441.57 (55 MPa) 49
34. Deviatorial stress vs strain: URL-5 442.36 (55 MPa) 50
35. Deviatorial stress vs strain: URL-6 374.22 (5 MPa) 51
36. Deviatorial stress vs strain: URL-6 392.04 (5 MPa) 52
37. Deviatorial stress vs strain: URL-6 373.69 (10 MPa) 53
38. Deviatorial stress vs strain: URL-6 391.25 (10 MPa) 54
39. Deviatorial stress vs strain: URL-6 391.48 (25 MPa) 55
40. Deviatorial stress vs strain: URL-6 391.71 (25 MPa) 56
41. Deviatorial stress vs strain: URL-6 374.85 (50 MPa) 57
42. Deviatorial stress vs strain: URL-6 392.27 (50 MPa) 58

INTRODUCTION

As part of the Nuclear Fuel Waste Management Program, a study has been carried out to determine if significant stress release is occurring in rock samples during coring and if this is having any effect on results obtained in the laboratory.

To accomplish this, specimens were selected from various depths (see Table 1) and were subjected to the folowing mechanical property tests:

1. Zero pressure and confined velocity measurements
2. Uniaxial compression tests
3. Brazilian tensile tests
4. Triaxial compression tests.

An additional objective of the Brazilian tensile tests was to determine if any discernible anisotropy exists in terms of tensile strength by testing adjacent samples along mutually perpendicular axes.

The purpose of this report is to provide a summary of the data obtained from these tests and offer some preliminary observations. A detailed report is being prepared in which a more extensive treatment of the data compiled from this study and previous test programs will be provided.

Table 1 - Borehole and Horizon identification and major principal stresses

Borehole Identification	Horizon (m)	σ_1 (MPa)	σ_2 (MPa)	σ_3 (MPa)	Overburden Pressure $\sigma_v = \rho gz$ (MPa) (ρ = 2.65 gm/cc)
URL-2	1080.14 - 1082.65	128.44	67.88	28.96	28.15
URL-5	441.65 - 443.07	52.82	27.77	12.00	11.52
URL-6	373.68 - 375.15	44.76	23.57	10.23	9.75
URL-6	391.18 - 392.40	46.77	24.60	10.65	10.19

IDENTIFICATION OF SPECIMENS AND TESTS

Mechanical property tests were conducted on 63 samples originating from boreholes URL-2, URL-5 and URL-6. The samples are generally described as granitic. A more complete geological description may be found in Wong et al. (1). Table 2 provides information on the dimensions, density and location of the 63 specimens. The following mechanical properties were determined:

1. Young's modulus
2. Poisson's ratio
3. Uniaxial compressive strength
4. Triaxial compressive strength
5. Brazilian tensile strength
6. Dynamic Young's modulus (confined and unconfined).

DESCRIPTION OF TEST MEASUREMENTS

Sample preparation and test measurements were carried out to conform with CANMET's Pit Slope Manual standards (2) and ASTM specifications (3).

Uniaxial Compressive Strength

For details on the uniaxial test procedure the reader is referred to CANMET Technical Data 303410-M01/78 (4). The two Phillips PR9302 Strain Bridges and the Mosely Autograph 2FRA X-Y recorder were replaced by two Bruel and Kjaer Type 1526 Strain Indicators and a Hewlett Packard 7046B X-Y recorder to measure and record the axial and transverse strain.

Triaxial Compressive Strength

Ambient temperature triaxial compression measurements were conducted utilizing CANMET's high temperature and pressure triaxial compression equipment (5).

Test samples with an approximate L/D ratio of 2.8 were encapsulated in an annealed copper jacket with dimensions close to that of the test specimen. The specimen jacket assembly was then sealed at alternate ends with a hardened steel ring over a tapered platen and a loading piston.

Table 2 - Dimensions and density of specimens

Specimen No.		Dimensions (mm) Length	Diameter	Density (gm/cc)
URL-2	1080.14	125.49	44.79	2.629
	1080.27	23.56	45.06	2.619
	1080.29	20.92	45.04	2.612
	1080.32	96.44	45.08	2.618
	1080.41	125.72	44.61	2.631
	1080.55	96.02	45.03	2.627
	1080.63	120.75	44.52	2.625
	1080.78	23.28	45.03	2.620
	1080.80	23.22	45.03	2.627
	1080.83	94.90	45.03	2.629
	1080.93	126.64	44.49	2.624
	1081.06	95.92	45.03	2.625
	1081.49	123.40	44.67	2.633
	1081.64	22.97	45.03	2.618
	1081.67	95.80	45.03	2.632
	1081.77	125.55	44.66	2.634
	1081.90	97.30	45.06	2.628
	1082.03	124.60	44.69	2.632
	1082.17	21.87	45.02	2.622
	1082.19	22.84	45.03	2.625
	1082.21	96.30	45.03	2.632
	1082.31	125.60	44.63	2.636
	1082.44	96.52	45.04	2.623
URL-5	441.57	122.05	44.63	2.656
	441.70	23.02	45.17	2.646
	441.73	22.91	45.17	2.648
	441.75	94.46	45.15	2.655
	441.85	125.59	44.53	2.661
	441.98	95.44	45.13	2.659
	442.08	24.16	45.16	2.647

Table 2 - Cont'd

Specimen No.		Dimensions (mm) Length	Diameter	Density (gm/cc)
URL-5	442.10	20.92	45.16	2.640
	442.13	126.59	44.64	2.656
	442.26	96.20	45.15	2.651
	442.36	125.61	44.64	2.656
	442.49	22.98	45.15	2.644
	442.51	22.90	45.15	2.648
	445.54	95.11	45.15	2.652
	442.64	125.63	44.64	2.658
	442.77	22.42	45.17	2.652
	442.80	24.08	45.16	2.650
	442.94	118.31	44.42	2.658
URL-6	373.69	118.03	44.45	2.633
	373.80	97.63	45.03	2.634
	374.22	125.50	44.28	2.630
	374.46	22.92	45.07	2.625
	374.48	22.63	45.06	2.650
	374.70	97.57	45.05	2.631
	374.80	21.27	45.07	2.624
	374.82	21.99	45.07	2.622
	374.85	124.76	44.47	2.648
	374.98	96.12	45.04	2.633
	391.20	22.96	45.04	2.625
	391.25	124.16	44.62	2.631
	391.38	95.30	45.02	2.625
	391.48	124.38	44.58	2.629
	391.61	95.29	45.01	2.648
	391.71	122.61	44.49	2.634
	391.84	22.07	45.00	2.630
	391.87	22.19	44.98	2.633
	391.89	97.65	44.98	2.630
	392.04	126.50	44.51	2.627
	392.17	96.14	45.00	2.598
	392.27	125.79	44.73	2.633

Two pairs of strain gauges oriented to measure axial deformation were connected in two half bridge configurations so that two independent axial deformational measurements could be obtained.

Readings were simultaneously recorded on the HP 7046B X-Y recorder and in 10 second intervals on a Fluke 2240 Data Logger. The data was reduced and a third degree equation fitted to the resulting stress/strain points. The derivative of this equation was used to estimate the tangent modulus at 50% of the failure strength. This method has been verified using the conventional graphical approach and been found to give slightly better accuracy (6).

Dilatational Velocity

Velocity tests were carried out with Terrametrics' Sonic Velocity Equipment using phenyl salicylate as a bonding agent. Zero pressure velocity measurements were obtained by simply attaching the pulsing heads to the specimen. For confined measurements, the specimens were placed in a Hoek cell and axial load was applied through the pulsing heads using a small hydraulic loading frame to the desired value. Confining pressure was then increased until equilibrium was reached. The compressional wave travel time was then measured with a Tektronix Type 555 Dual Beam Oscilloscope. The procedure was repeated for confining pessure ranging from 2 to 30 MPa.

Brazilian Tensile Strength

Brazilian tensile tests were conducted on the core using specimens with an approximate L/D ratio of 0.5. Samples were selected such that two specimens would be adjacent to one another along the core axis. One of the two samples was then loaded on the core reference line while the other was loaded perpendicular to it.

DATA SUMMARY

Table 3 summarizes the uniaxial compressive strength, deformational properties and zero pressure velocities for the samples tested uniaxially. Table 4 includes the confined velocity data and the corresponding dynamic Young's modulus values. The Brazilian tensile test results are listed in

Table 3 - Summary of uniaxial compressive strength, zero pressure velocity and deformation property data of specimens

Specimen No.		Length	Diameter	Young's Modulus (GPa)	Poisson's Ratio	Compressive Strength (MPa)	Zero Pressure Velocity (km/sec)
URL-2	1080.32*	96.44	45.08	51.58	0.30	198.42	2.53
URL-2	1080.55	96.02	45.03	51.82	0.22	189.84	2.45
URL-2	1080.83*	94.90	45.03	51.90	0.40	163.26	2.52
URL-2	1081.06	95.92	45.03	52.54	0.30	166.40	2.48
URL-2	1081.67	95.80	45.03	54.26	0.34	178.33	2.62
URL-2	1081.90*	97.30	45.06	51.78	0.36	162.41	2.86
URL-2	1082.21	96.30	45.03	51.99	0.43	160.12	2.88
URL-2	1082.44*	96.52	45.04	46.62	0.35	180.13	2.71
				$\bar{E}$ = 51.56	$\bar{\nu}$ = 0.34	$\bar{x}$ = 174.86	
				(σ = 2.17)	σ = .065	σ = 14.13	
URL-5	441.75*	94.46	45.15	56.06	0.31	226.73	3.70
URL-5	441.98	95.44	45.13	52.90	0.30	186.29	3.57
URL-5	442.26	96.20	45.15	56.69	0.27	223.60	3.64
URL-5	442.54*	95.11	45.15	56.63	0.29	199.87	3.83
				$\bar{E}$ = 55.57	$\bar{\nu}$ = 0.29	$\bar{x}$ = 209.12	
				σ = 1.80	σ = 0.017	σ = 14.13	
URL-6	373.80*	97.63	45.03	59.20	0.39	180.84	3.73
URL-6	374.70*	97.57	45.05	61.73	0.31	170.02	3.84
URL-6	374.98	96.12	45.04	58.54	0.33	203.98	3.76
URL-6	391.38*	95.30	45.02	55.52	0.32	196.63	3.71
URL-6	391.61	95.29	45.01	56.58	0.29	170.32	3.55
URL-6	391.89*	97.65	44.98	56.44	0.31	183.13	3.73
URL-6	392.17	96.14	45.00	58.23	0.30	147.76	3.47
				$\bar{E}$ = 58.03	$\bar{\nu}$ = 0.32	$\bar{x}$ = 178.95	
				σ = 2.09	σ = .033	σ = 18.65	

* Confined velocity measurements were conducted on these samples prior to testing

Table 4 - Combined velocity measurements

Sample No.:	URL-2 1080.32			URL-2 1080.83			URL-2 1081.90		
Young's Modulus:	51.58 GPa			51.90 GPa			51.78 GPa		
Confining Pressure (MPa)	Tp (μsec)	Vp (km/sec)	Dynamic Young's Modulus (GPa)	Tp (μsec)	Vp (km/sec)	Dynamic Young's Modulus (GPa)	Tp (μsec)	Vp (km/sec)	Dynamic Young's Modulus (GPa)
0	35.70	2.70	12.40	36.38	2.61	11.63	34.15	2.85	13.87
2	31.95	3.02	15.51	32.28	2.94	14.76	30.70	3.17	17.16
5	26.50	3.64	22.54	27.43	3.46	20.45	30.95	3.14	16.83
10	22.55	4.28	31.16	24.28	3.91	26.11	25.30	3.85	25.31
15	20.10	4.80	39.19	21.73	4.37	32.62	21.45	4.54	35.19
20	19.10	5.05	43.38	19.98	4.75	38.54	20.45	4.76	38.69
25	18.40	5.24	46.71	19.03	4.99	42.53	19.15	5.08	44.06
30	17.85	5.40	49.61	18.23	5.21	46.36	18.35	5.30	47.96
Average		4.27	33.31		4.03	29.13		4.09	29.88

Table 4 - Cont'd

Sample No.:	URL-2 1082.44			URL-5 441.75			URL-5 442.54		
Young's Modulus:	46.62 GPa			56.06 GPa			56.63 GPa		
Confining Pressure (MPa)	Tp (μsec)	Vp (km/sec)	Dynamic Young's Modulus (GPa)	Tp (μsec)	Vp (km/sec)	Dynamic Young's Modulus (GPa)	Tp (μsec)	Vp (km/sec)	Dynamic Young's Modulus (GPa)
0	35.78	2.70	12.42	24.46	3.86	30.18	24.56	3.87	30.31
2	31.98	3.02	15.54	26.06	3.62	26.54	30.66	3.10	19.45
5	28.53	3.38	19.47	21.16	4.46	40.29	29.41	3.21	20.86
10	25.63	3.77	24.22	20.41	4.63	43.42	24.41	3.90	30.78
15	24.13	4.00	27.27	18.86	5.01	50.84	23.01	4.09	33.86
20	21.48	4.49	34.36	18.41	5.13	53.31	22.16	4.29	37.25
25	20.28	4.76	38.61	17.76	5.32	57.33	21.36	4.45	40.08
30	19.58	4.93	41.42	17.01	5.55	62.40	20.76	4.58	42.46
Average		3.88	26.66		4.70	45.54		3.94	31.88

Table 4 - Cont'd

Sample No.:	URL-6 373.80			URL-6 374.70			URL-6 391.38		
Young's Modulus:	59.20 GPa			61.73 GPa			55.52 GPa		
Confining Pressure (MPa)	Tp (μsec)	Vp (km/sec)	Dynamic Young's Modulus (GPa)	Tp (μsec)	Vp (km/sec)	Dynamic Young's Modulus (GPa)	Tp (μsec)	Vp (km/sec)	Dynamic Young's Modulus (GPa)
0	27.76	3.52	22.80	26.63	3.66	24.63	26.70	3.57	21.87
2	25.51	3.83	27.00	25.03	3.90	27.97	26.45	3.60	22.00
5	23.06	4.23	32.93	23.73	4.11	31.06	23.70	4.02	29.26
10	20.36	4.80	42.41	20.98	4.65	39.76	20.40	4.67	36.68
15	19.26	5.07	47.31	19.83	4.92	44.51	19.00	5.02	45.12
20	18.31	5.33	52.29	18.93	5.15	48.77	18.35	5.19	48.36
25	17.41	5.61	57.93	18.73	5.36	52.82	17.80	5.35	52.60
30	17.06	5.72	60.22	17.63	5.53	56.22	17.15	5.56	57.02
Average		4.76	42.86		4.66	40.72		4.62	39.01

Table 4 - Cont'd

Sample No.:	URL-6 391.89
Young's Modulus:	56.44 GPa

Confining Pressure (MPa)	Tp (μsec)	Vp (km/sec)	Dynamic Young's Modulus (GPa)	Tp (μsec)	Vp (km/sec)	Dynamic Young's Modulus (GPa)	Tp (μsec)	Vp (km/sec)	Dynamic Young's Modulus (GPa)
0	28.33	3.45	21.87						
2	28.23	3.46	22.00						
5	24.48	3.99	29.26						
10	21.78	4.48	36.88						
15	19.93	4.90	44.12						
20	19.03	5.13	48.36						
25	18.23	5.35	52.60						
30	17.53	5.57	57.02						
Average		4.54	39.01						

Table 5 with the specimen dimensions, weight and density. Table 6 lists the specimen dimensions and results of the triaxial measurements. Figure 1 shows a plot of tangent modulus of elasticity vs confining pressure for boreholes URL-2, 5 and 6.

BASIC DATA

Figure 2 through 20 are the axial and circumferential stress-strain curves from which the elastic properties of the nineteen specimens tested uniaxially were determined. The final load value on the specimens was used to determine the uniaxial compressive strength.

The elastic properties for the triaxial samples were determined from Fig. 21 through 42. The "x's" represent actual data points while the line represents the fitted third degree equation.

SUMMARY AND CONCLUSIONS

The uniaxial modulus of elasticity showed a marked decrease with depth ranging from 58.03 GPa for the upper URL-6 horizon (373.68 - 393.404) to 51.56 GPa for the lower URL-2 horizon (1080.14 - 1082.65). It appears, however, that the observed moduli converge to between 65 and 70 GPa under confining pressures of approximately 20 MPa or greater (Fig. 1).

Zero pressure velocity measurements also exhibited a decrease with depth. The dynamic modulus determined using the zero pressure velocity data differed considerably from those obtained from the uniaxial tests. It was possible, however, to achieve dynamic moduli exceeding the static moduli found uniaxially in four of the six upper horizon specimens when confining pressure was applied. This behaviour was not observed for the lower URL-2 horizon over the confining pressure range used for the measurements.

The lowest average Brazilian tensile strength (6.98 MPa) was observed for the lower URL-2 horizon specimens. The URL-5 specimens exhibited the highest tensile strength with an average value of 9.74 MPa while samples obtained from the URL-6 borehole had an average strength of 7.97 MPa. There was no discernible trend involving the two core orientations used for tests.

Table 5 - Brazilian tensile test results

Specimen No.	Length (mm)	Diameter (mm)	Weight (gm)	Density (gm/cc)	Test* Orientation	Tensile Strength (MPa)
URL-2 1080.27	23.56	45.06	98.41	2.619		6.79
1080.29	20.92	45.04	87.06	2.612		6.94
1080.78	23.28	45.03	97.15	2.620		7.12
1080.80	23.22	45.03	97.15	2.627		6.63
1081.64	22.97	45.03	95.77	2.618		7.46
1082.17	21.87	45.02	91.28	2.622		7.69
1082.19	22.84	45.03	95.47	2.625		6.22
URL-5 441.70	23.02	45.17	97.61	2.646		9.31
441.73	22.91	45.17	97.21	2.648		9.87
442.08	24.16	45.16	102.42	2.647		9.97
442.10	20.92	45.16	88.48	2.640		8.75
442.49	22.98	45.15	97.29	2.644		10.51
442.51	22.90	45.15	97.10	2.648		9.95
442.77	22.42	45.17	95.27	2.652		10.10
442.80	24.08	45.16	102.20	2.650		9.46
URL-6 374.46	22.92	45.07	95.95	2.625		8.71
374.48	22.63	45.06	94.72	2.625		8.66
374.80	21.27	45.07	89.03	2.624		8.46
374.82	21.99	45.07	91.98	2.622		8.39
391.60	22.96	45.04	96.04	2.265		5.96
391.84	22.07	45.00	92.33	2.630		7.82
391.87	22.19	44.98	92.83	2.633		7.80

*Adjacent specimens were located along the core reference line (⌒) and perpendicular to the core reference line (⊖)

Table 6 - Results of triaxial tests on URL specimens

Specimen Identification	Length (mm)	Diameter (mm)	Confining Pressure σ_3 (MPa)	Temperature (°C)	Axial Stress Rate (MPa/sec)	Total Axial Strain (%)	Triaxial Strength (GPa)	Tangent Modulus (GPa)
URL-2 1080.14	125.49	44.79	10.0	21°	0.68	0.732	345	60.16
URL-2 1081.77	125.55	44.66	10.0	21°	0.87	0.725	356	60.55
URL-2 1080.41	125.72	44.61	35.0	21°	0.74	1.076	601	65.44
URL-2 1081.49	123.40	44.67	35.0	21°	0.71	0.904	532	67.04
URL-2 1080.93	126.64	44.49	50.0	21°	0.76	1.127	674	67.46
URL-2 1082.31	125.60	44.63	50.0	21°	1.14	1.102	636	64.57
URL-2 1080.63*	120.75	44.52	50.0	21°	0.95	1.012	651	66.74
URL-2 1082.03*	124.60	44.69	50.0	21°	1.10	1.205	638	64.11
URL-2 1080.63	120.75	44.52	70.0	21°	0.98	0.907	727**	66.71
URL-2 1082.03	124.60	44.69	70.0	21°	0.95	1.001	713**	66.27

* Samples were previously cycled at σ_3 = 70.0 MPa

** Triaxial strengths were estimated using failure strengths determined at σ_3 = 50.0 MPa

Table 6 - Cont'd

Specimen Identification	Length (mm)	Diameter (mm)	Confining Pressure σ_3 (MPa)	Temperature (°C)	Axial Stress Rate (MPa/sec)	Total Axial Strain (%)	Triaxial Strength (GPa)	Tangent Modulus (GPa)
URL-5 442.13	126.59	44.64	15.0	21°	0.89	0.861	419	58.67
URL-5 442.94	118.31	44.42	15.0	21°	0.45	0.781	367	59.34
URL-5 441.85	125.59	44.53	30.0	21°	0.84	1.107	534	60.99
URL-5 442.64	125.63	44.64	30.0	21°	1.06	1.046	539	61.25
URL-5 441.57	122.05	44.63	55.0	21°	0.61	0.498	317*	62.94
URL-5 442.36	125.61	44.64	55.0	21°	1.06	1.270	708	63.80

*Failure occurred along a pre-existing fracture plane

Table 6 - Cont'd

Specimen Identification	Length (mm)	Diameter (mm)	Confining Pressure σ_3 (MPa)	Temperature (°C)	Axial Stress Rate (MPa/sec)	Total Axial Strain (%)	Triaxial Strength (GPa)	Tangent Modulus (GPa)
URL-6 374.22	125.50	44.28	5.0	21°	0.60	0.570	303	56.59
URL-6 392.04	126.50	44.51	5.0	21°	0.58	0.528	288	63.28
URL-6 373.69	118.03	44.55	10.0	21°	0.54	0.608	344	66.32
URL-6 391.25	124.16	44.62	10.0	21°	0.54	0.663	361	65.42
URL-6 391.48	124.38	44.58	25.0	21°	0.73	0.824	488	68.87
URL-6 391.71	122.61	44.49	25.0	21°	0.46	0.916	488	63.36
URL-6 374.85	124.76	44.47	50.0	21°	0.79	1.014	597	69.21
URL-6 392.79	125.79	44.73	50.0	21°	0.90	1.087	629	68.52

Both the uniaxial deformational properties and zero pressure velocities indicate that some type of stress relief mechanism is occurring which results in the lower unconfined results observed in samples originating from lower URL-2 horizon. However, the stress relief effect on the elastic deformational properties appears to be damped with the application of a maximum confining pressure of approximately 20 MPa. The confining pressure required to eliminate these effects does not appear to be great although it does seem to increase slightly with an increase in sample depth.

The Brazilian tests showed little preference as to core orientation with six sets of samples having greater tensile strength when loaded along the core reference line and four when loaded perpendicular to it. This would seem to indicate little or no anisotropy in the samples at least along these two axes.

REFERENCES

1. Wong, A.S. "Modal analyses of URL-1, URL-2, URL-5 and URL-6 extended engineering samples"; Mining Research Laboratories, CANMET, in prep.

2. CANMET Pitslope Manual "Mechanical properties, chapter 3".

3. "Standard test method for triaxial compressive strength of undrained rock core samples without pore pressure measurements"; Designation D 2664-67 (reapproved 1974); American Society for Testing and Materials; Philadelphia, Pa., pp 327-330; 1974.

4. Annor, A. and Geller, L. "Technical data 303410 M01 to M06/78"; Mining Research Laboratories, CANMET; 1978.

5. Annor A., Miles, P., Kapeller, F. and Larocque, G. "High temperature and pressure triaxial compression tests on rock samples from Pinawa and Creighton mines"; Division Report ERP/MRL 80-102(TR); CANMET, Energy, Mines and Resources, Canada; 1980.

6. Jackson, R. "High temperature and pressure triaxial compression tests on rock sampes from URL-6"; Mining Research Laboratories, CANMET, in prep.

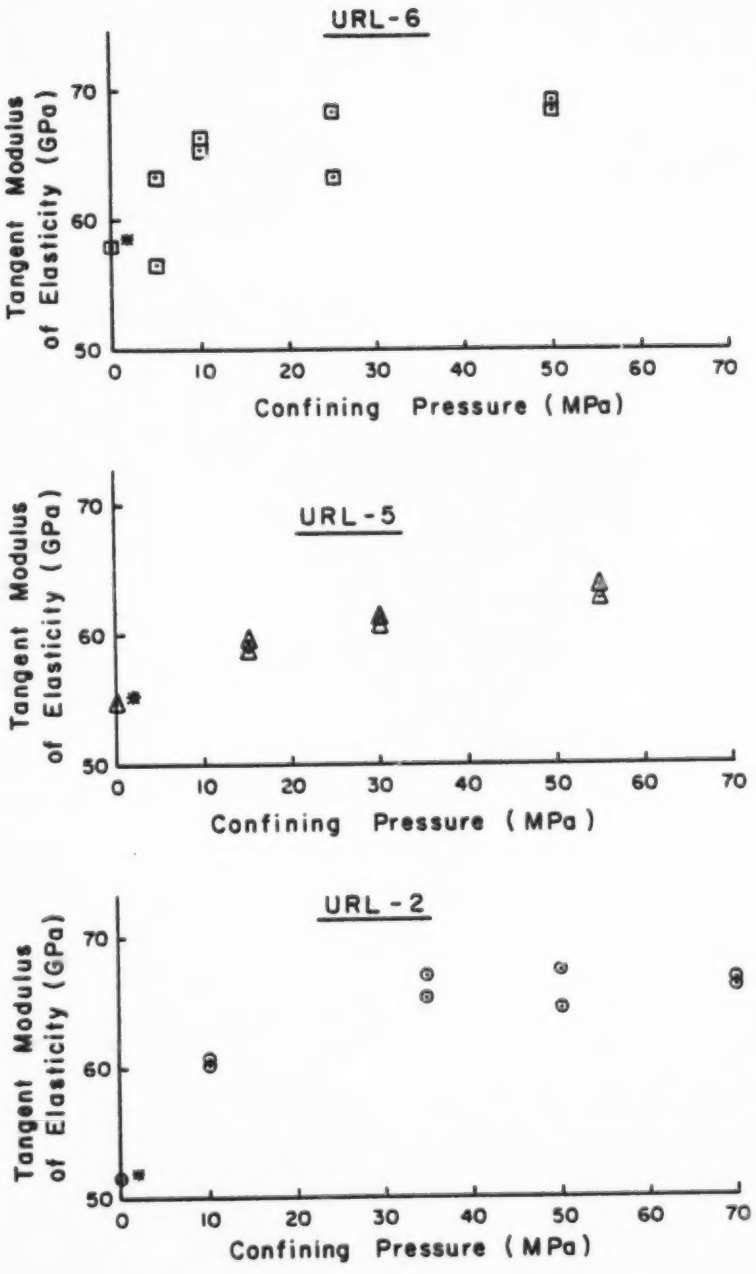

* – represents an average of moduli determined from uniaxial results

Fig. 1 – Tangent modulus of elasticity vs confining pressure: Boreholes URL-2, 5 & 6

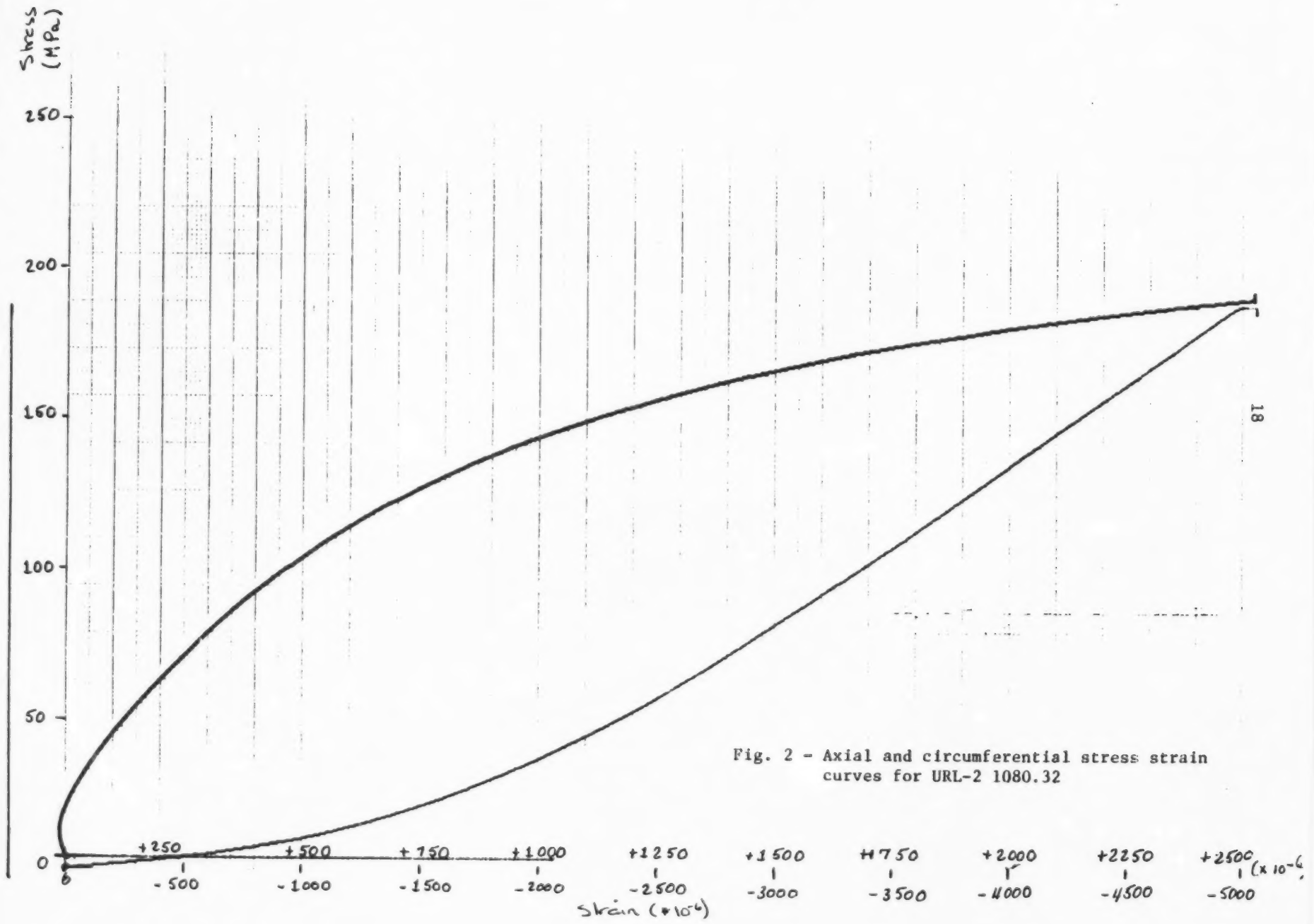

Fig. 2 - Axial and circumferential stress strain curves for URL-2 1080.32

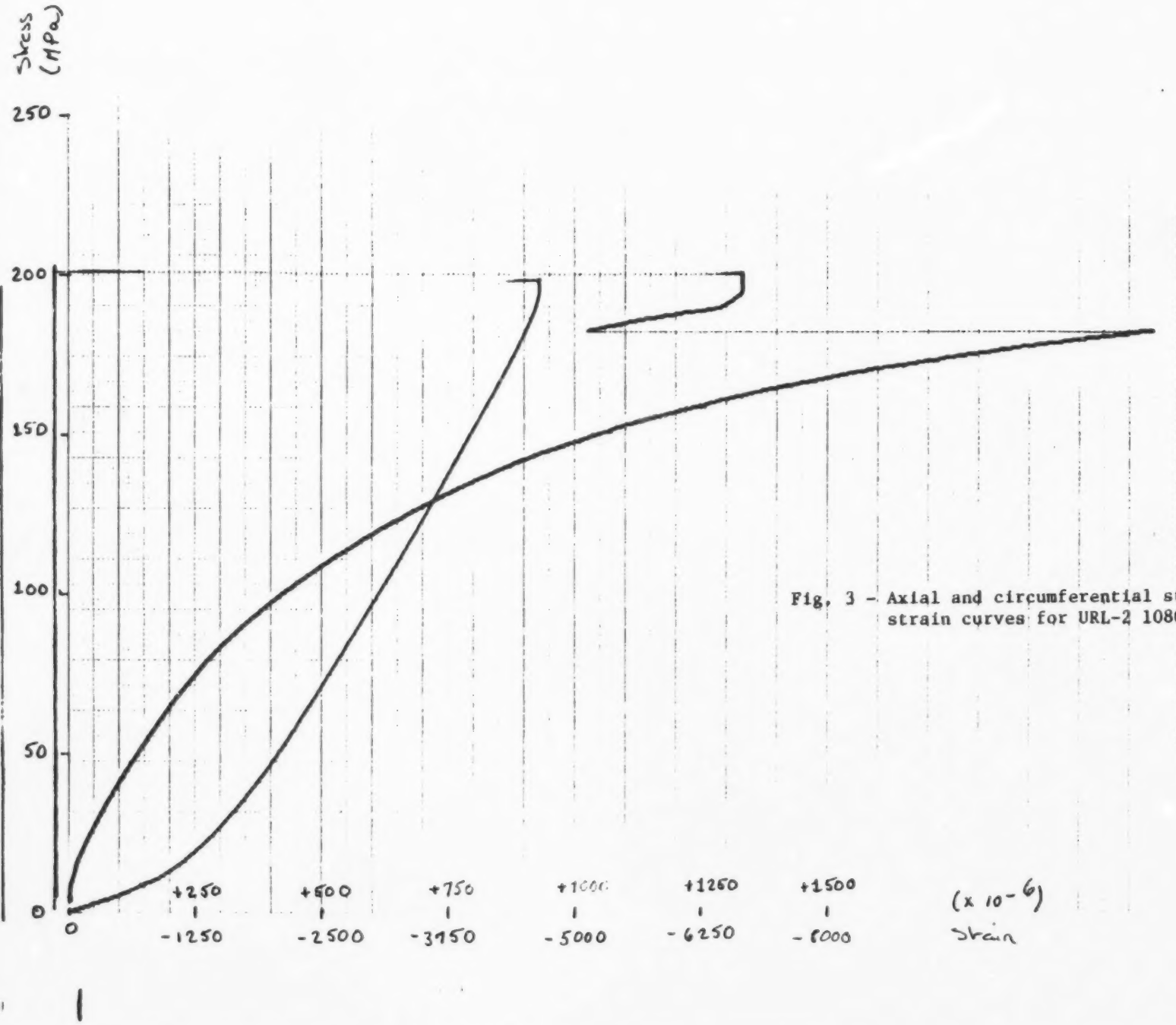

Fig. 3 - Axial and circumferential stress strain curves for URL-2 1080.55

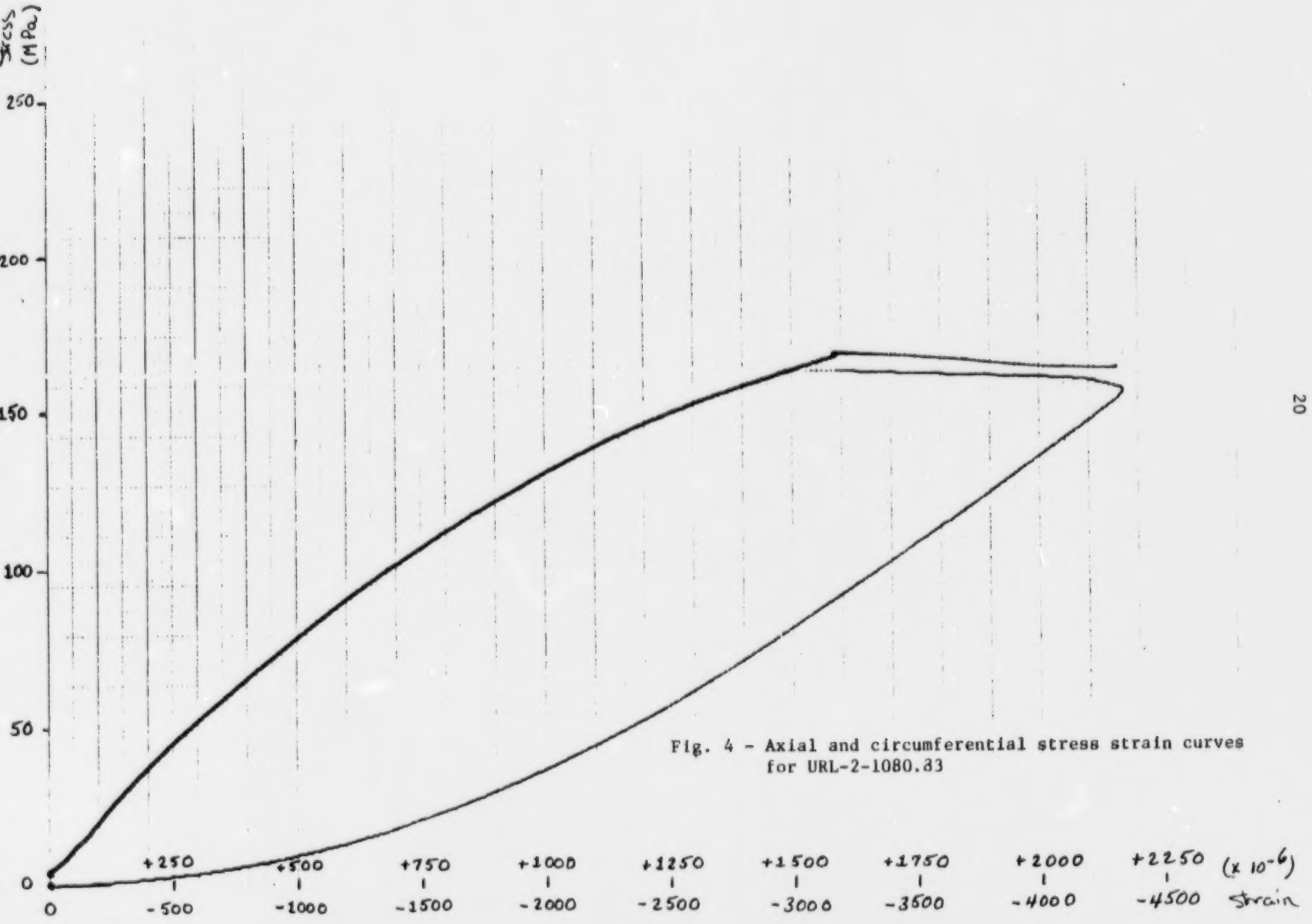

Fig. 4 - Axial and circumferential stress strain curves for URL-2-1080.33

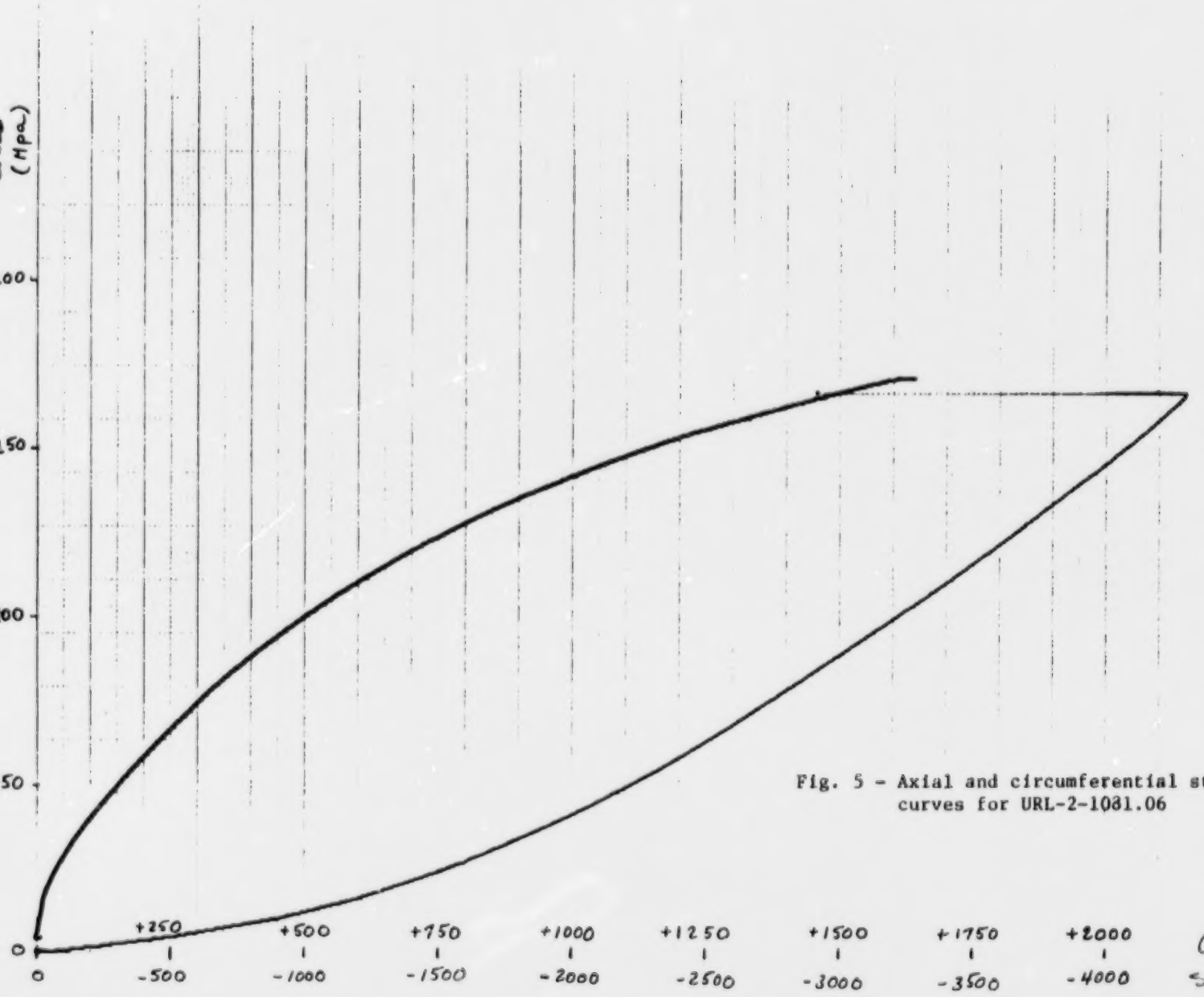

Fig. 5 - Axial and circumferential stress strain curves for URL-2-1081.06

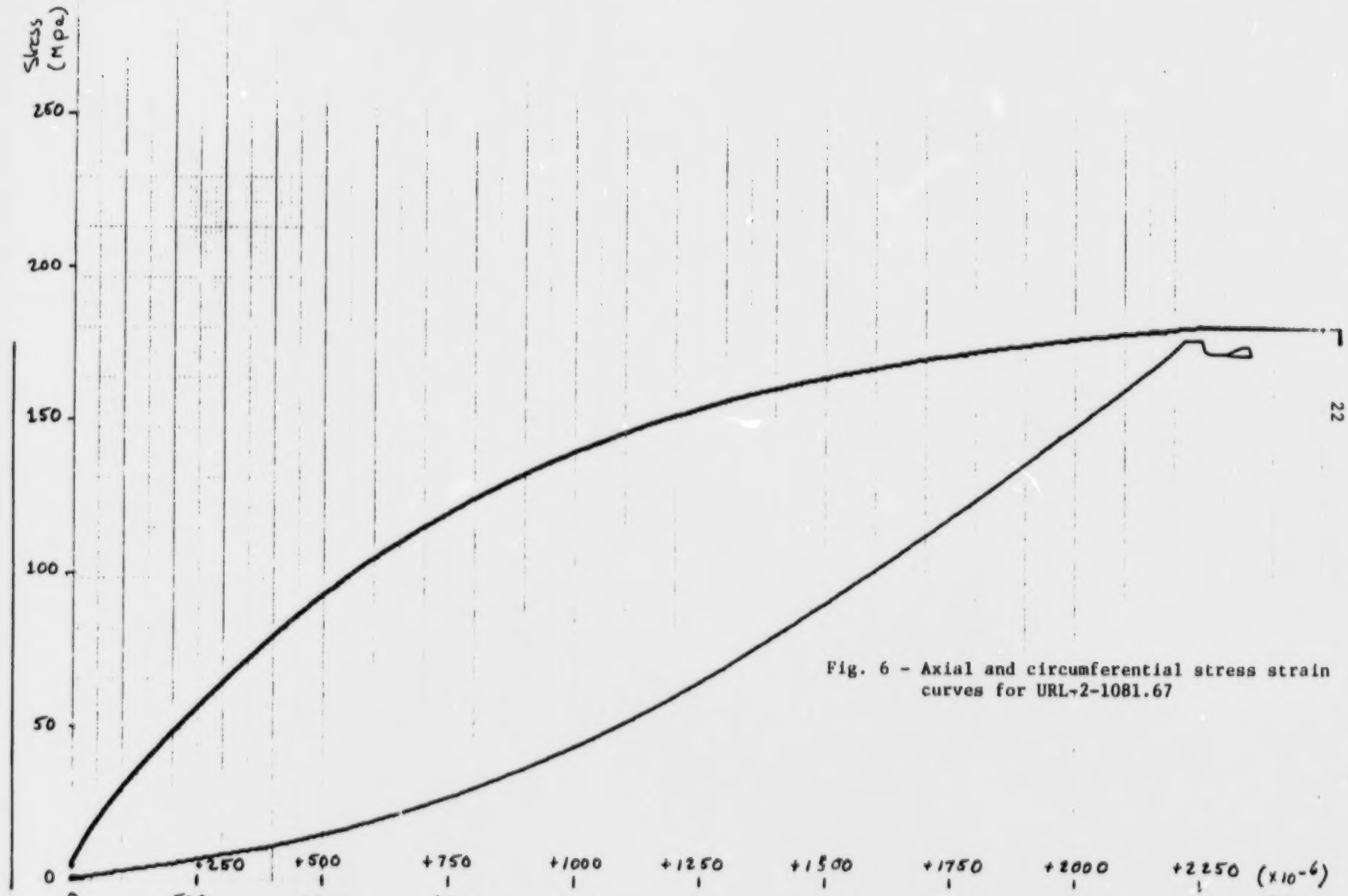

Fig. 6 - Axial and circumferential stress strain curves for URL-2-1081.67

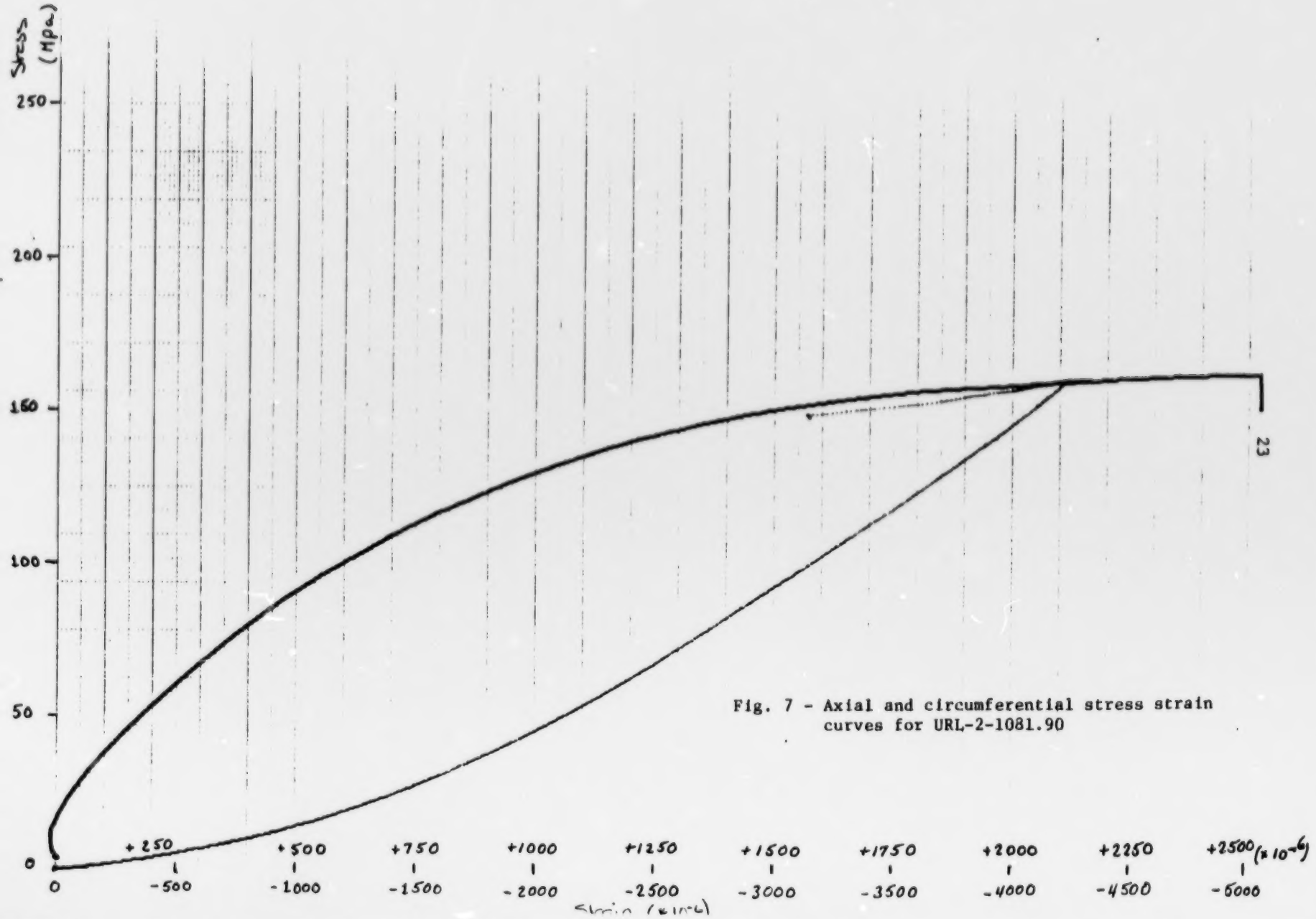

Fig. 7 - Axial and circumferential stress strain curves for URL-2-1081.90

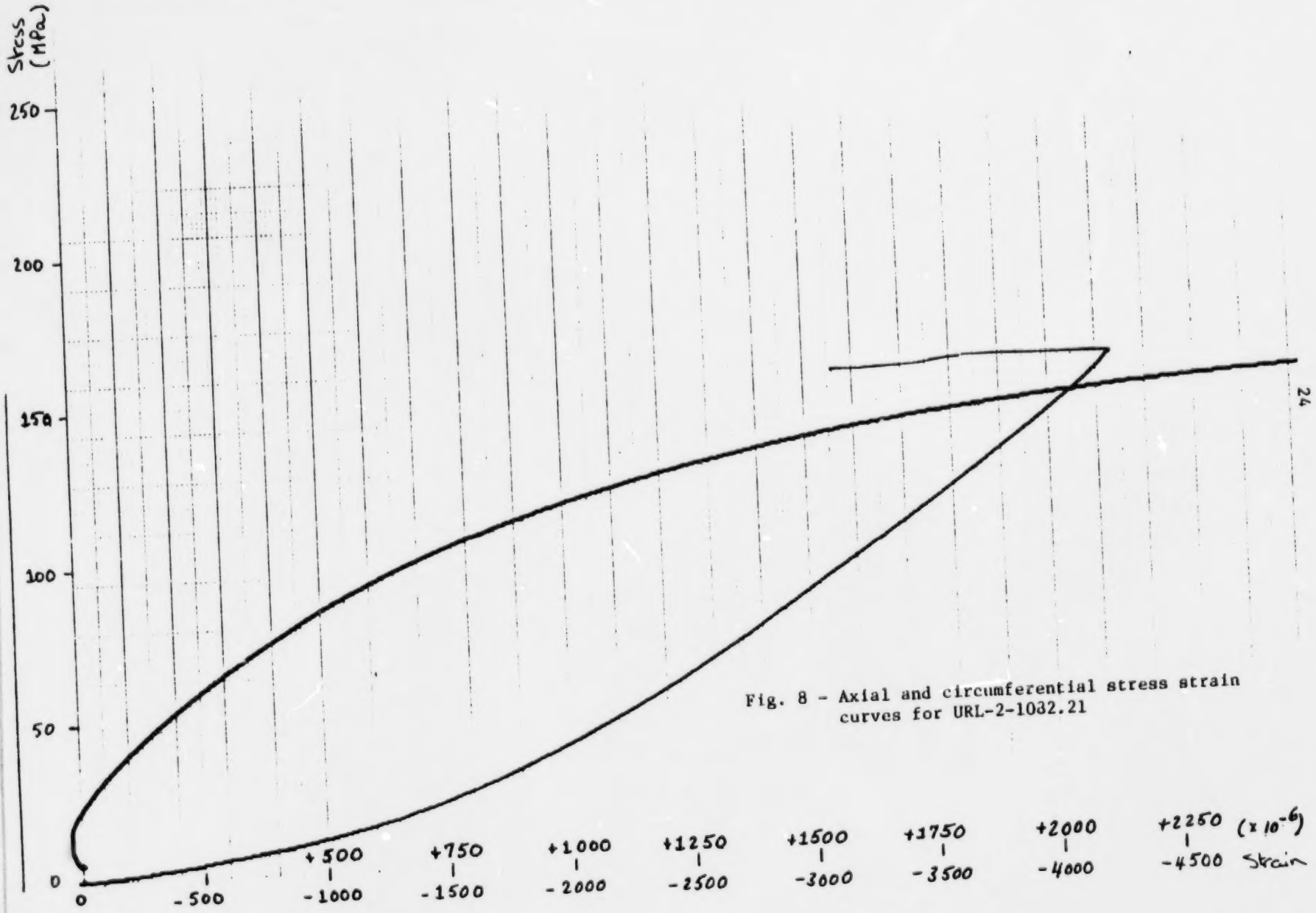

Fig. 8 - Axial and circumferential stress strain curves for URL-2-1032.21

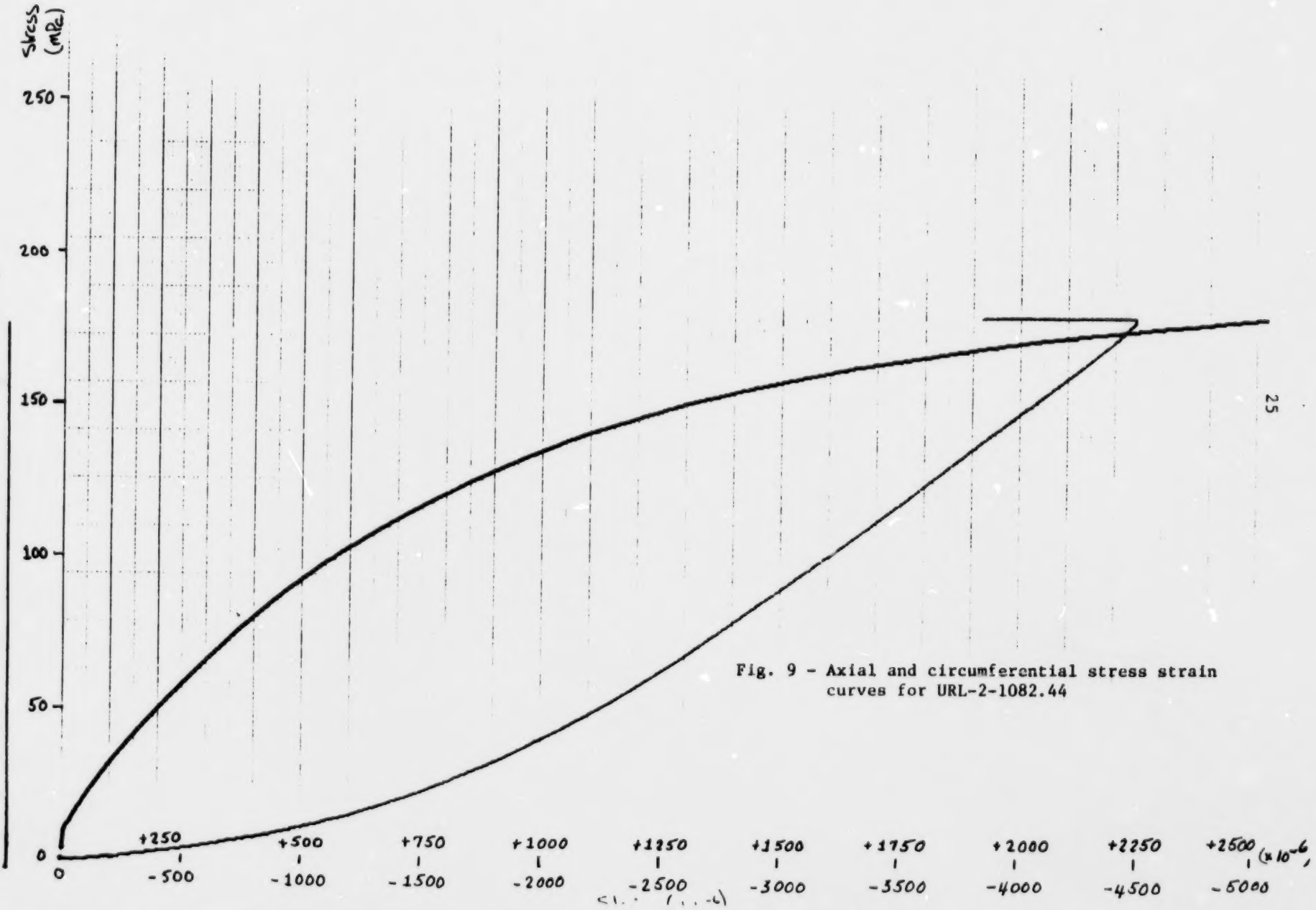

Fig. 9 - Axial and circumferential stress strain curves for URL-2-1082.44

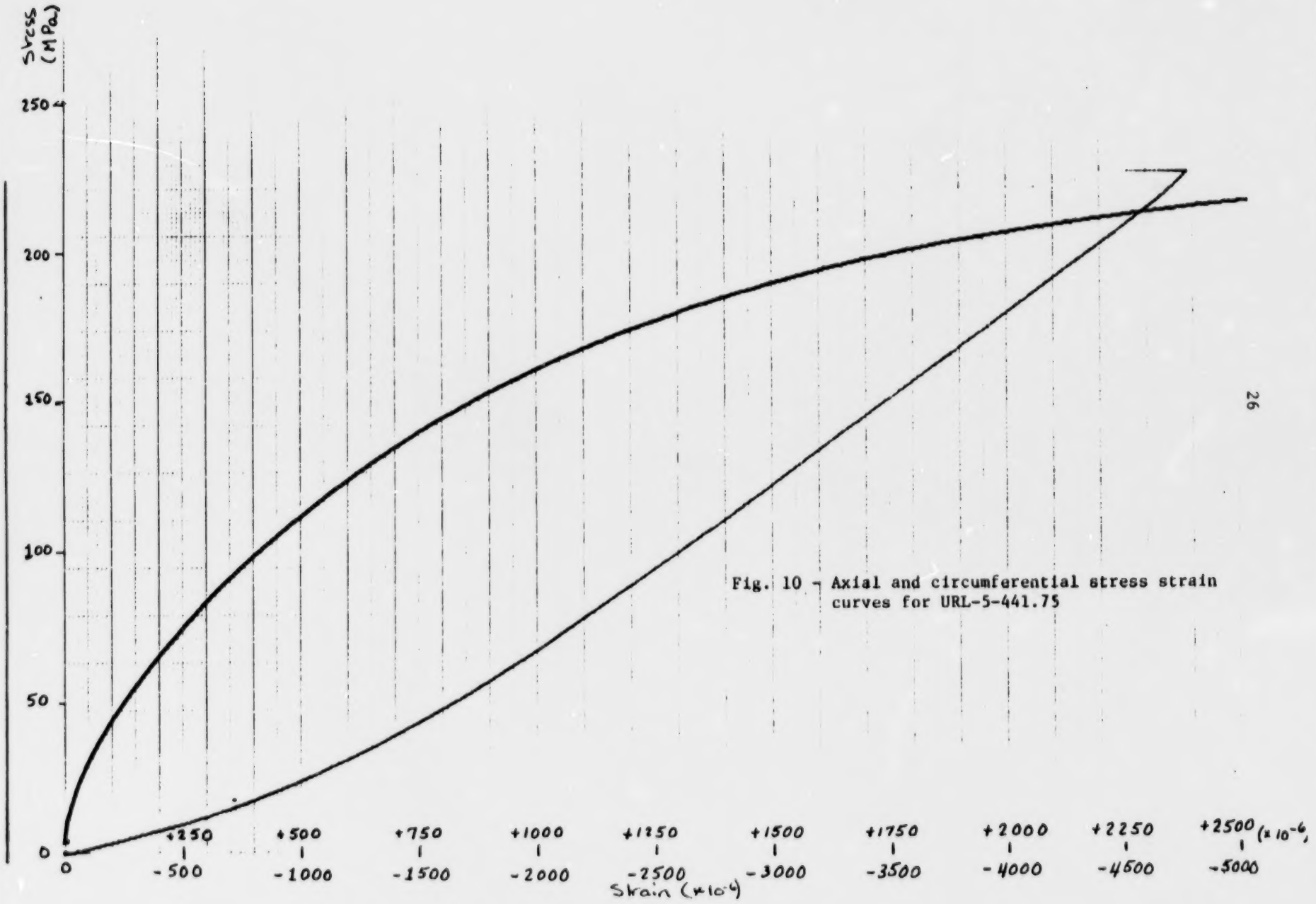

Fig. 10 - Axial and circumferential stress strain curves for URL-5-441.75

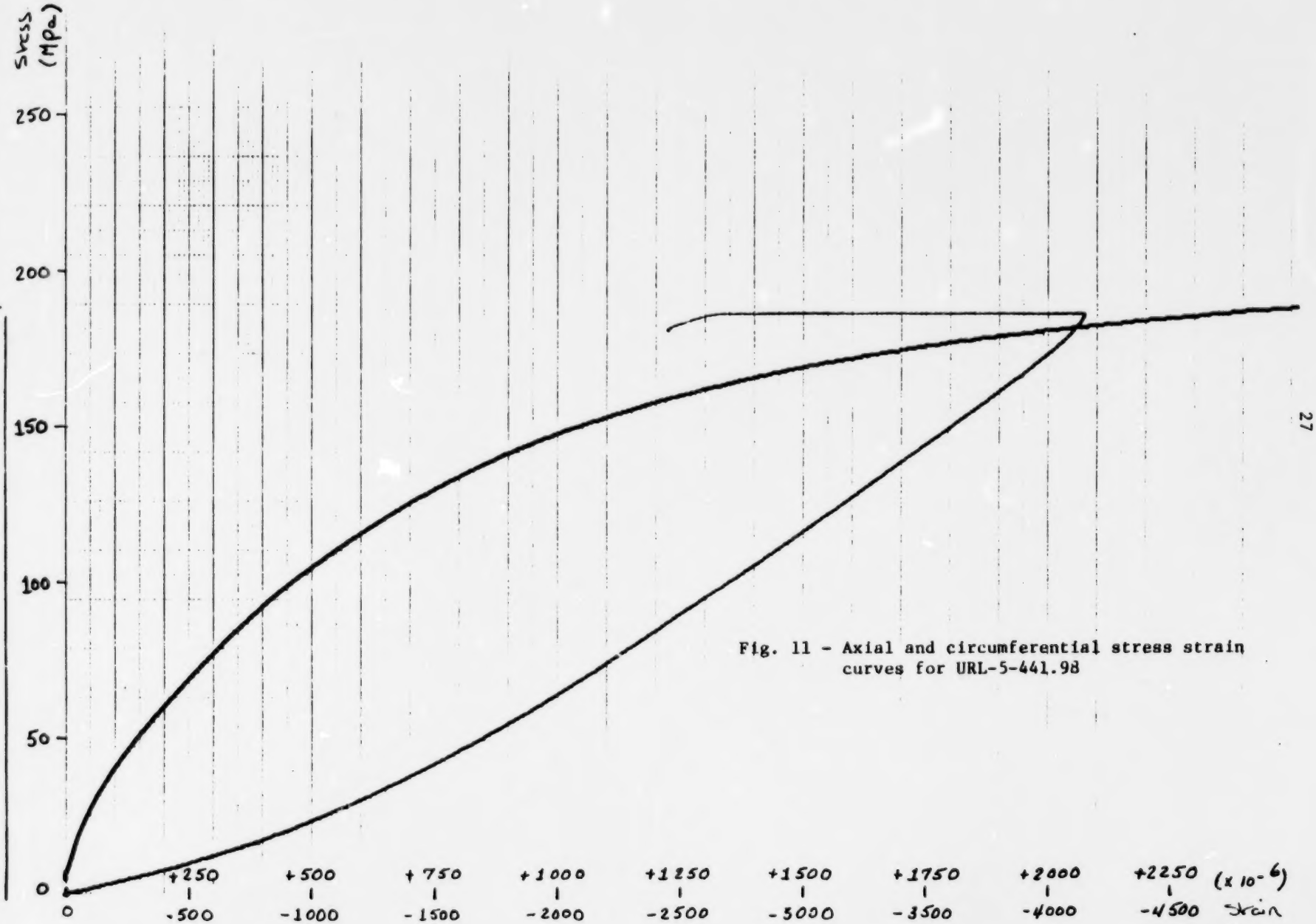

Fig. 11 - Axial and circumferential stress strain curves for URL-5-441.98

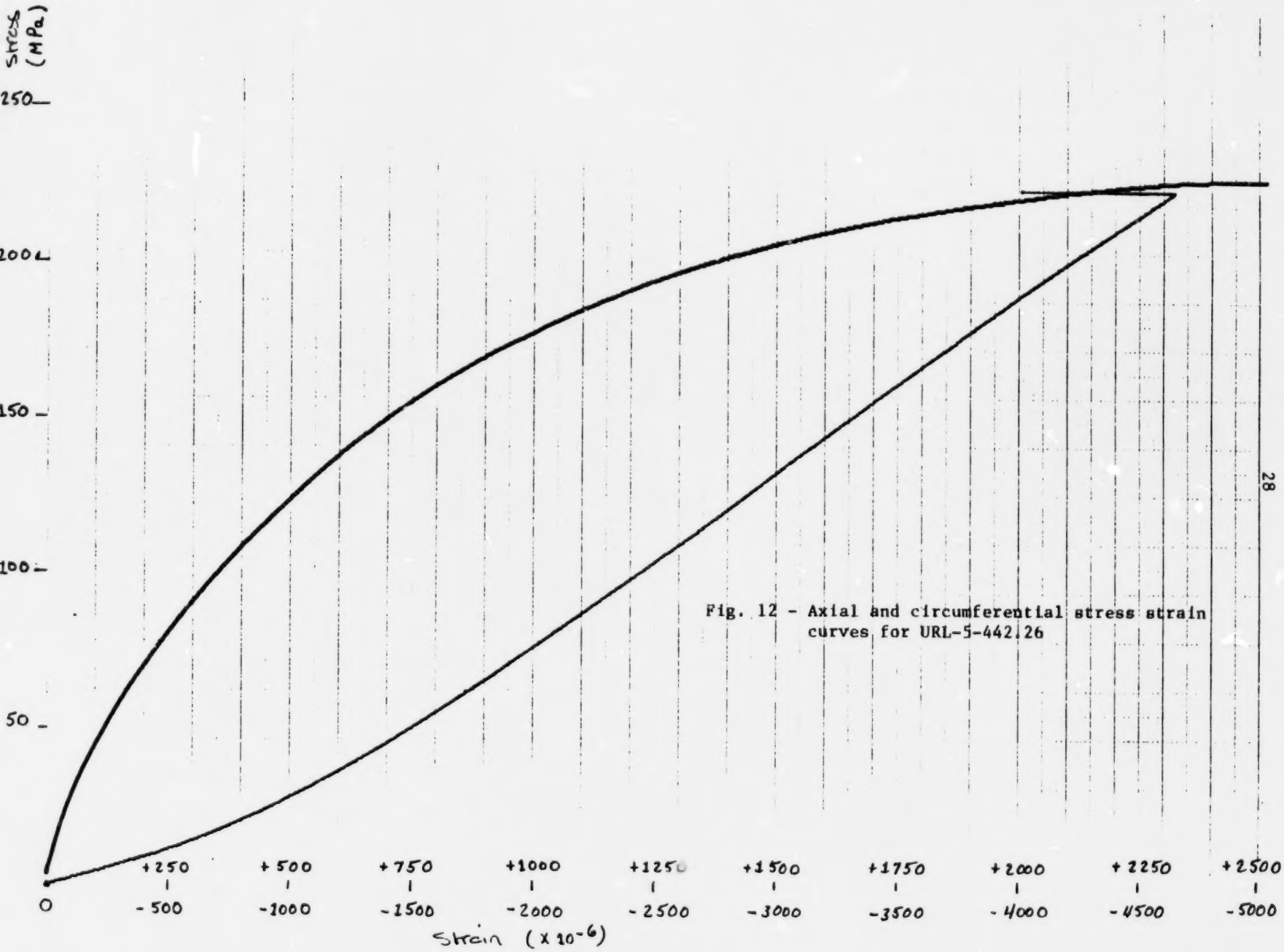

Fig. 12 - Axial and circumferential stress strain curves for URL-5-442.26

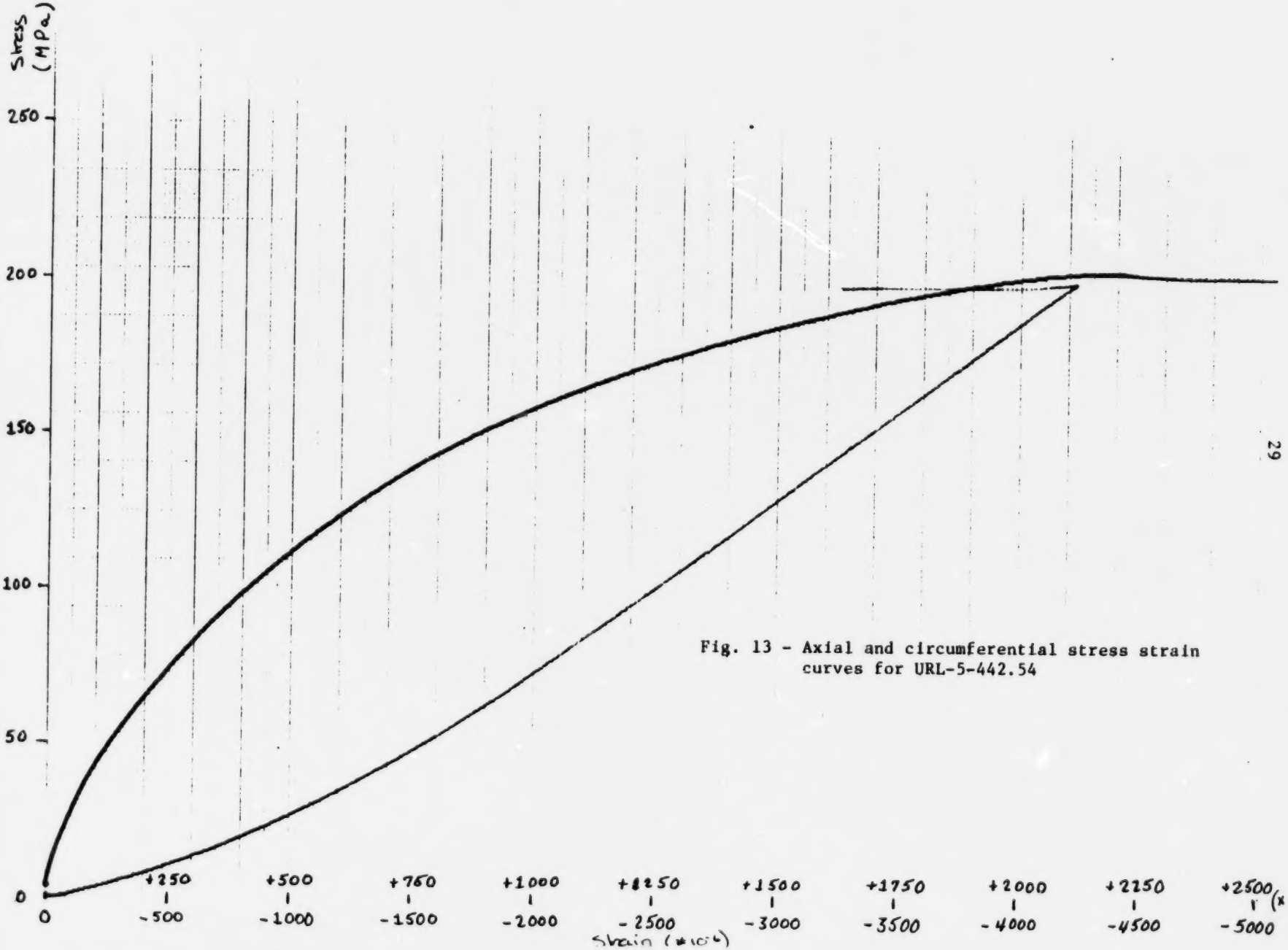

Fig. 13 - Axial and circumferential stress strain curves for URL-5-442.54

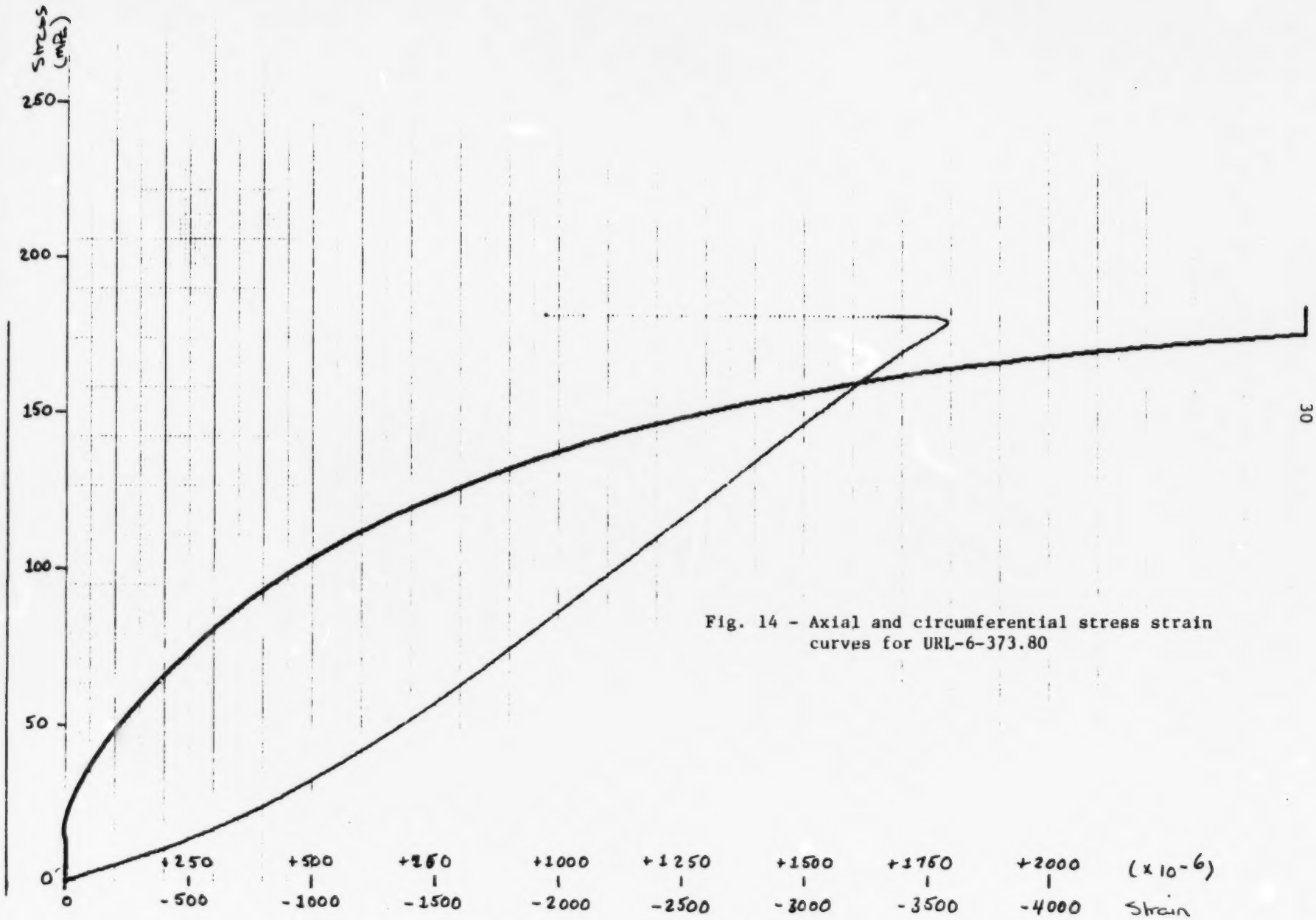

Fig. 14 - Axial and circumferential stress strain curves for URL-6-373.80

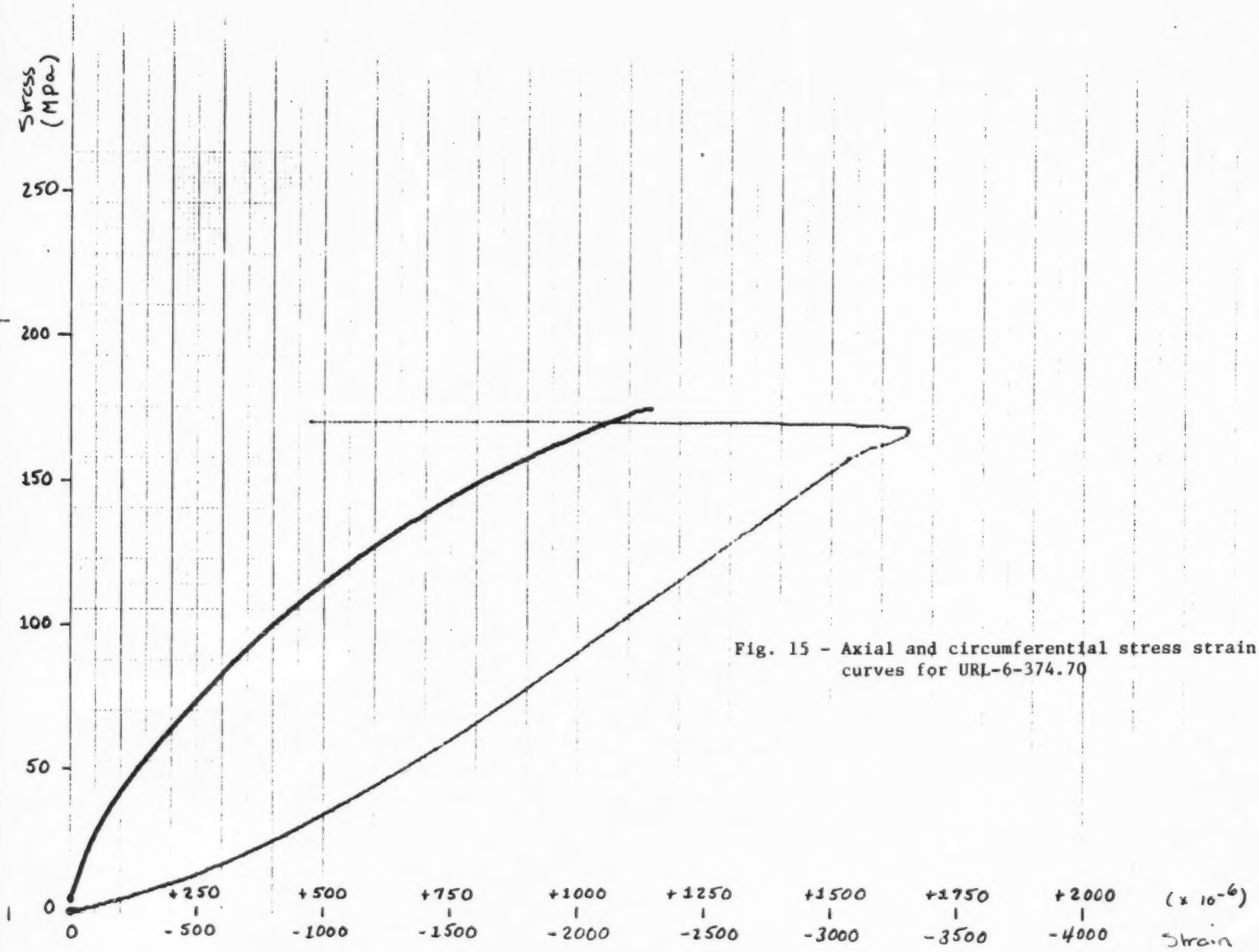

Fig. 15 - Axial and circumferential stress strain curves for URL-6-374.70

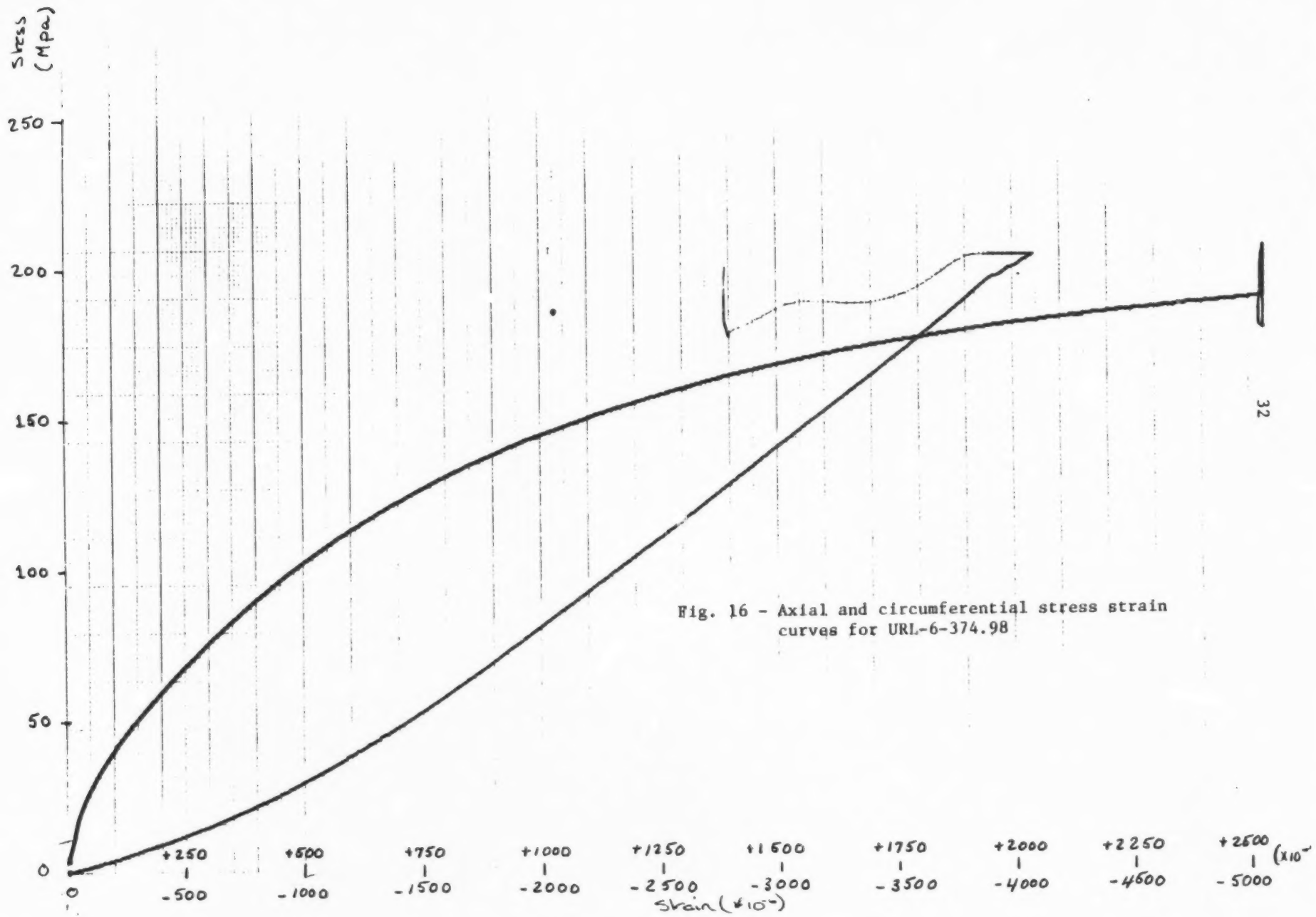

Fig. 16 - Axial and circumferential stress strain curves for URL-6-374.98

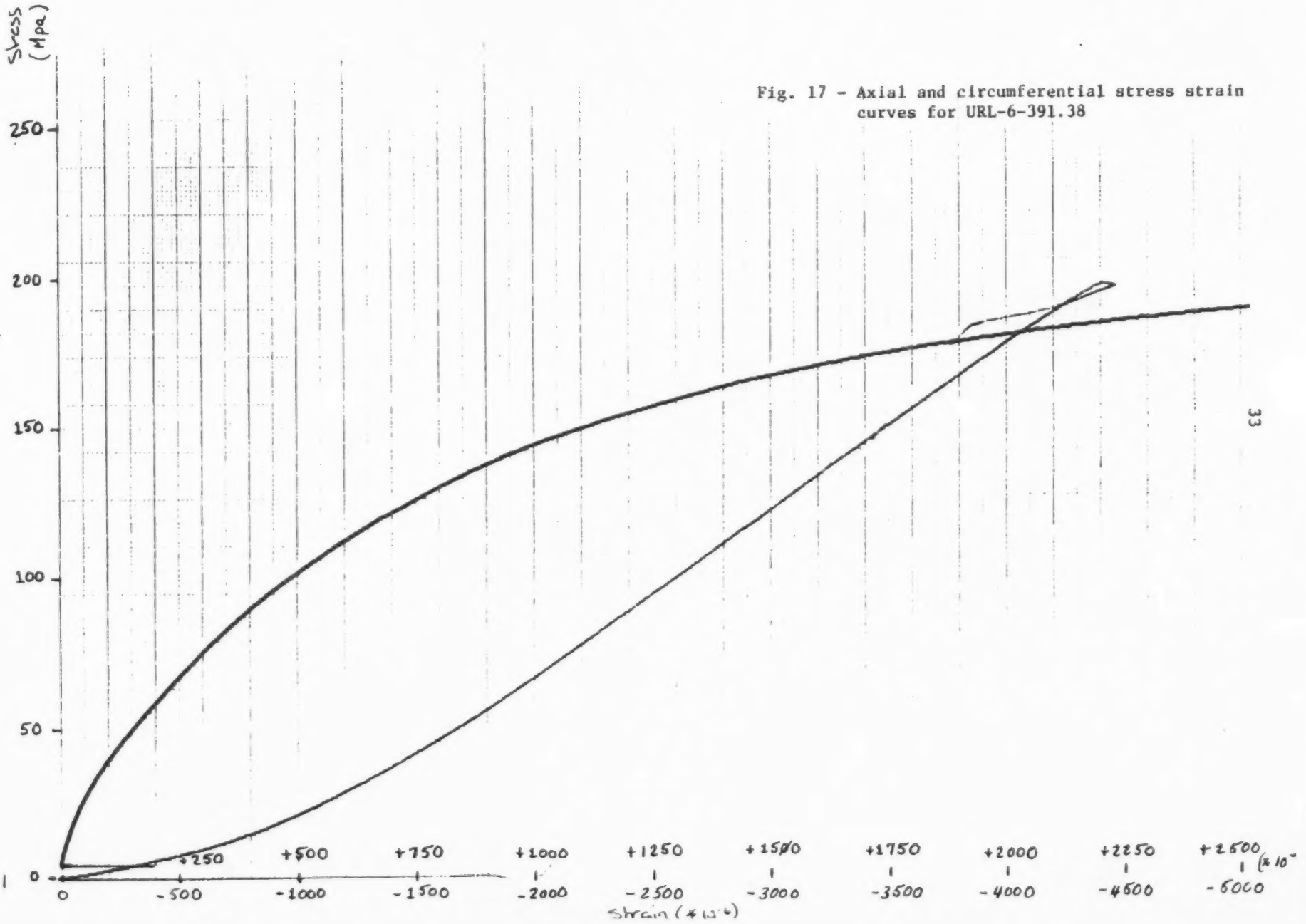

Fig. 17 - Axial and circumferential stress strain curves for URL-6-391.38

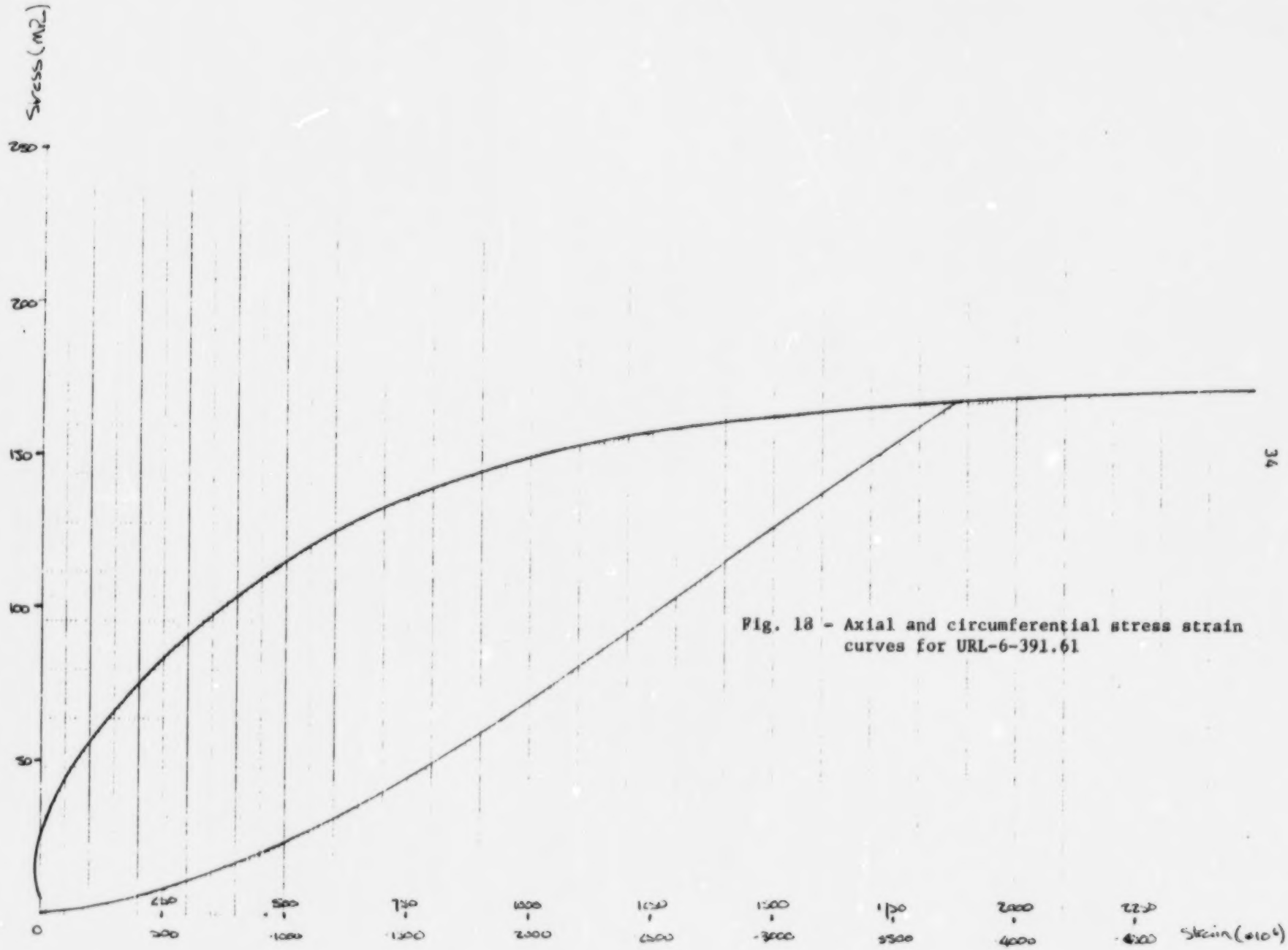

Fig. 18 - Axial and circumferential stress strain curves for URL-6-391.61

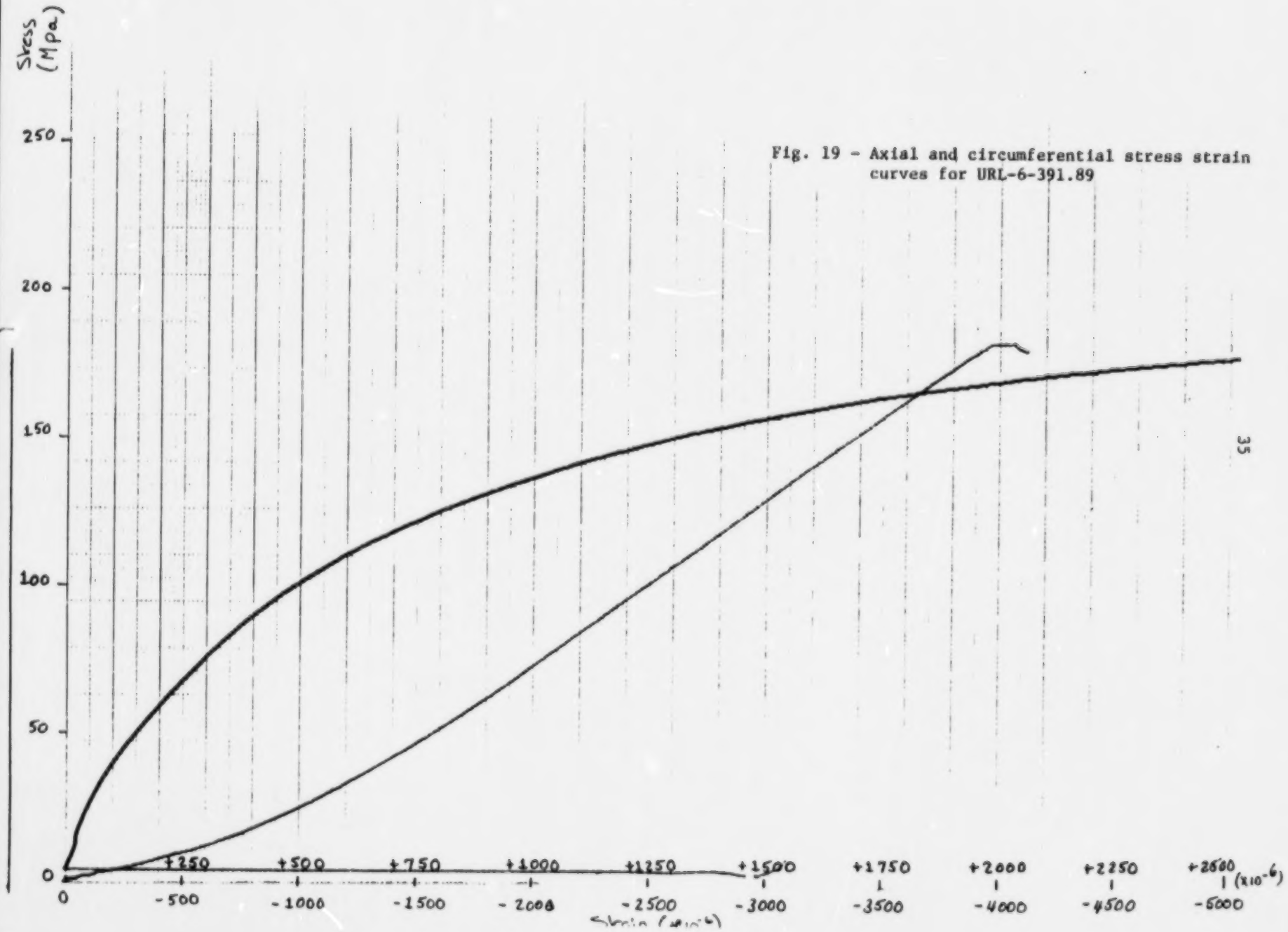

Fig. 19 - Axial and circumferential stress strain curves for URL-6-391.89

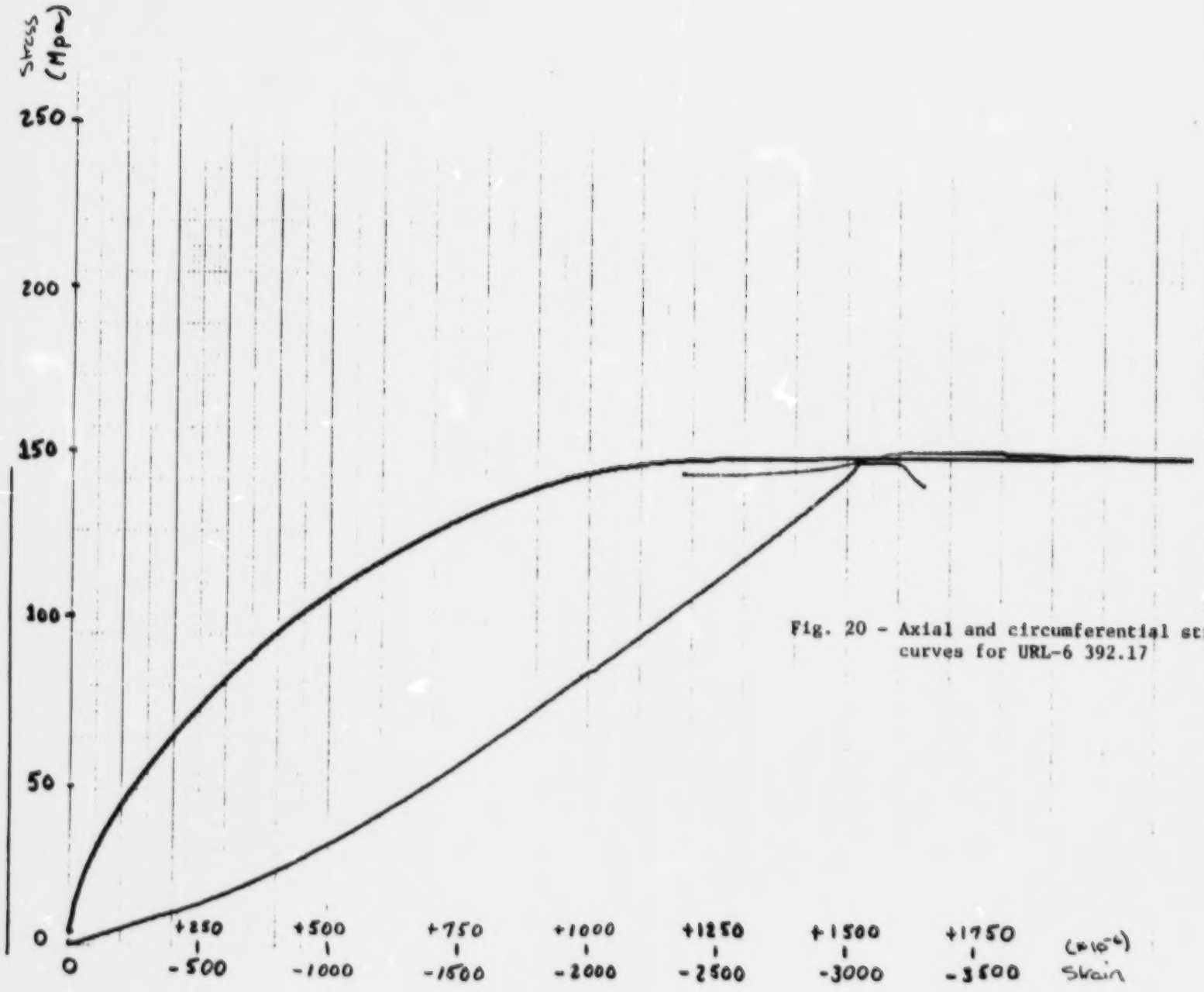

Fig. 20 - Axial and circumferential stress strain curves for URL-6 392.17

FIG. 21: DEVIATORIAL STRESS VS STRAIN: URL2 1080.14 (10.0 MPa)

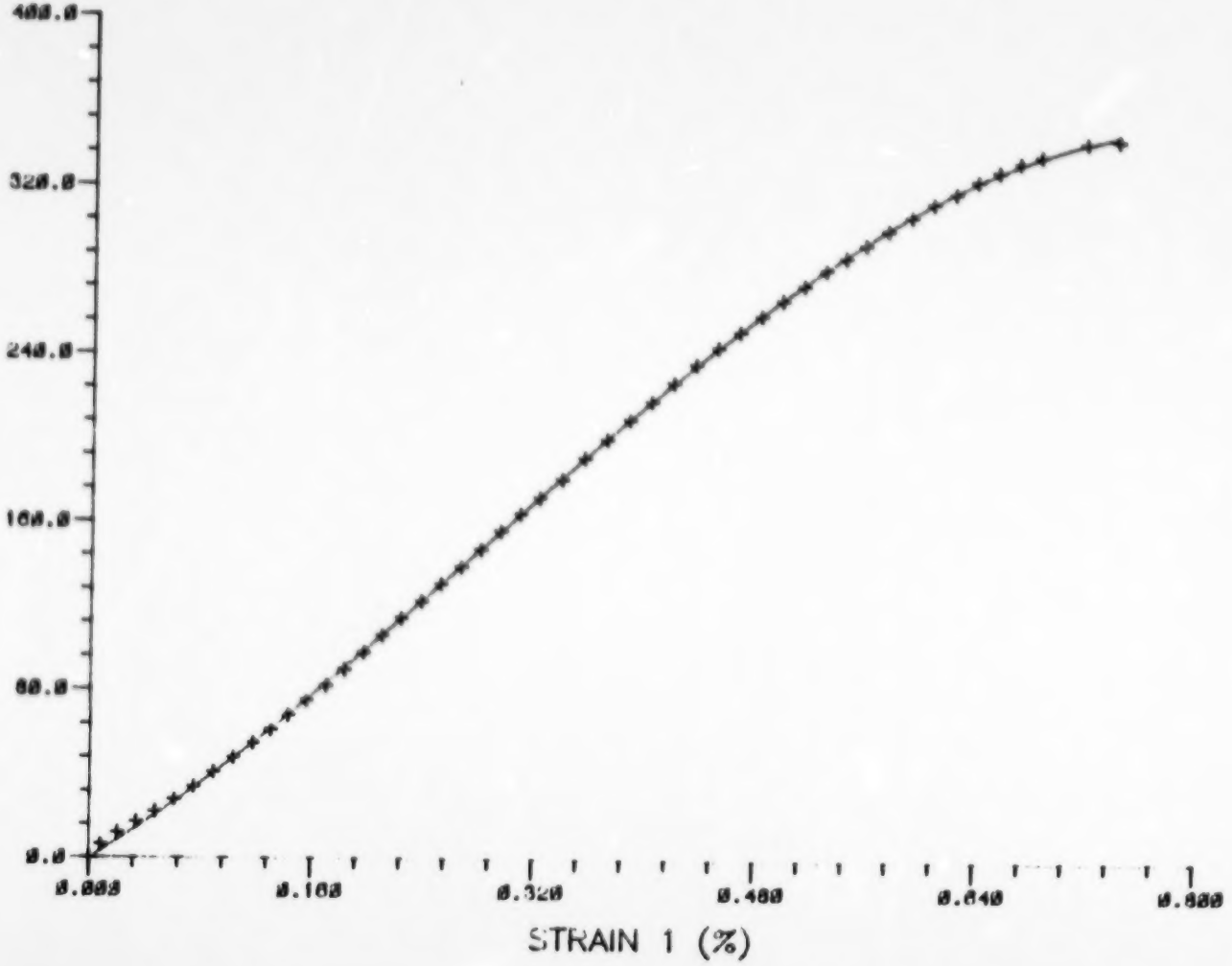

FIG. 22: DEVIATORIAL STRESS VS STRAIN: URL2 1081.77 (10.0 MPa)

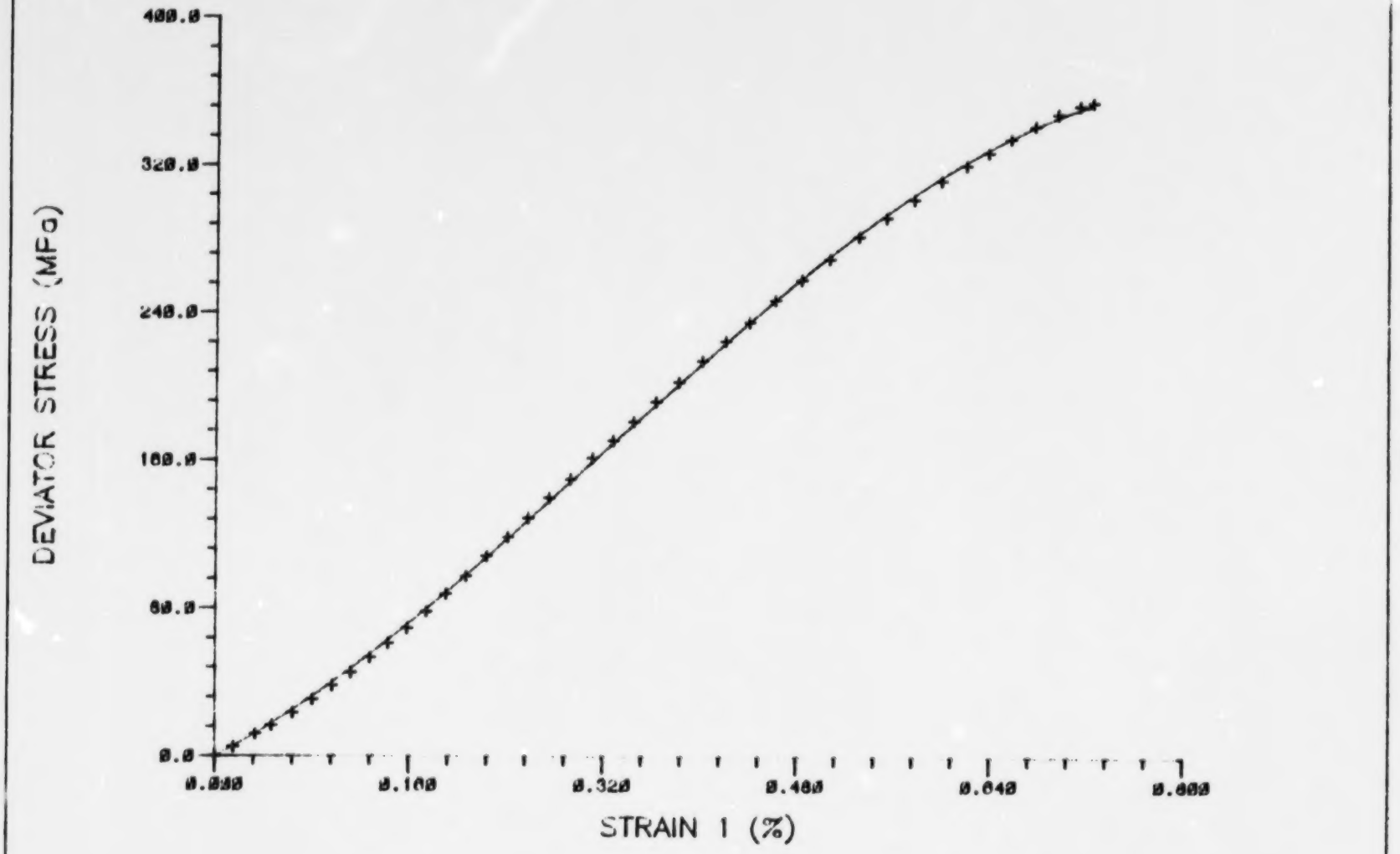

FIG. 23: DEVIATORIAL STRESS VS STRAIN: URL2 1080.41 (35.0 MPa)

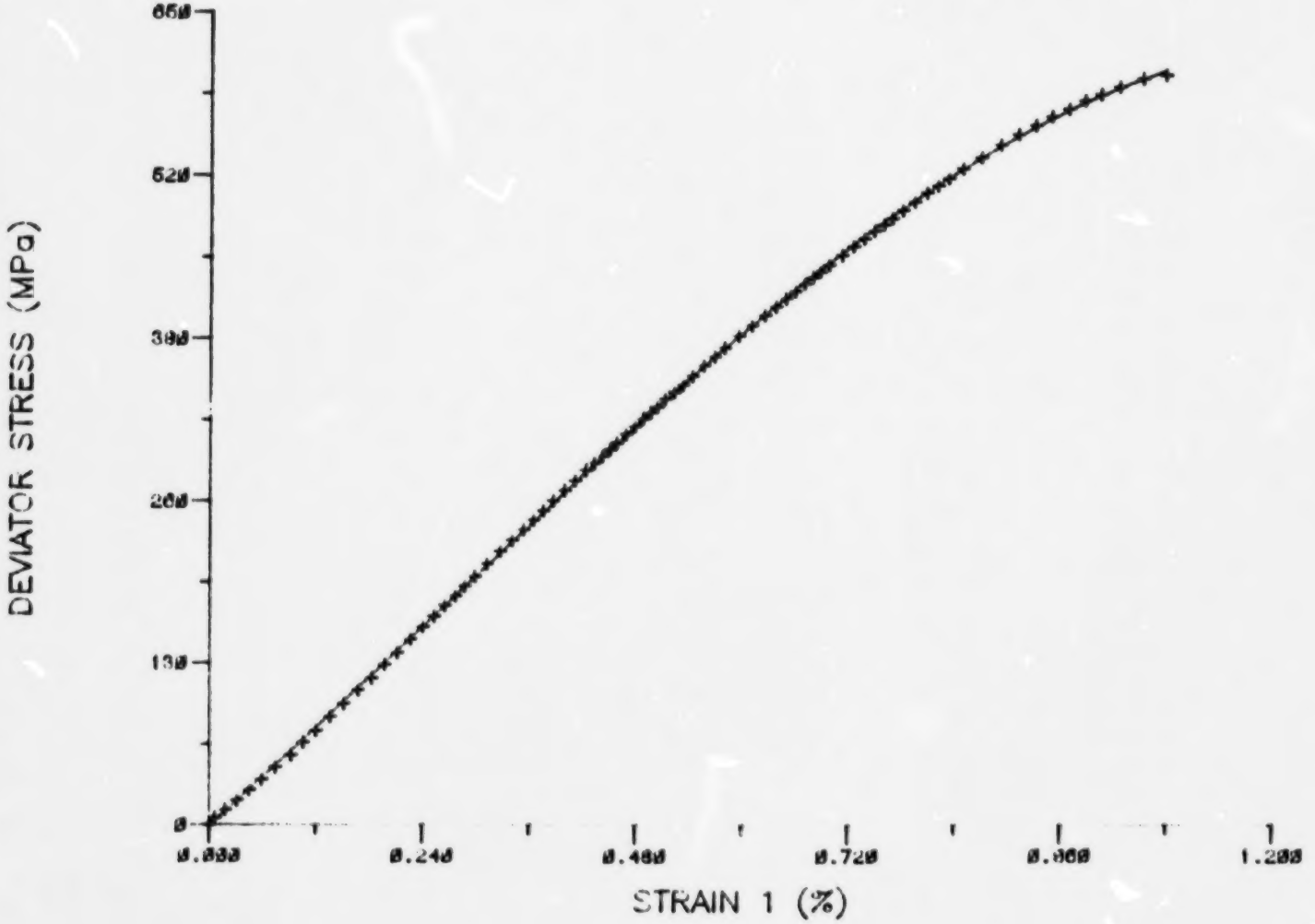

FIG. 24: DEVIATORIAL STRESS VS STRAIN: URL2 1081.49 (35.0 MPa)

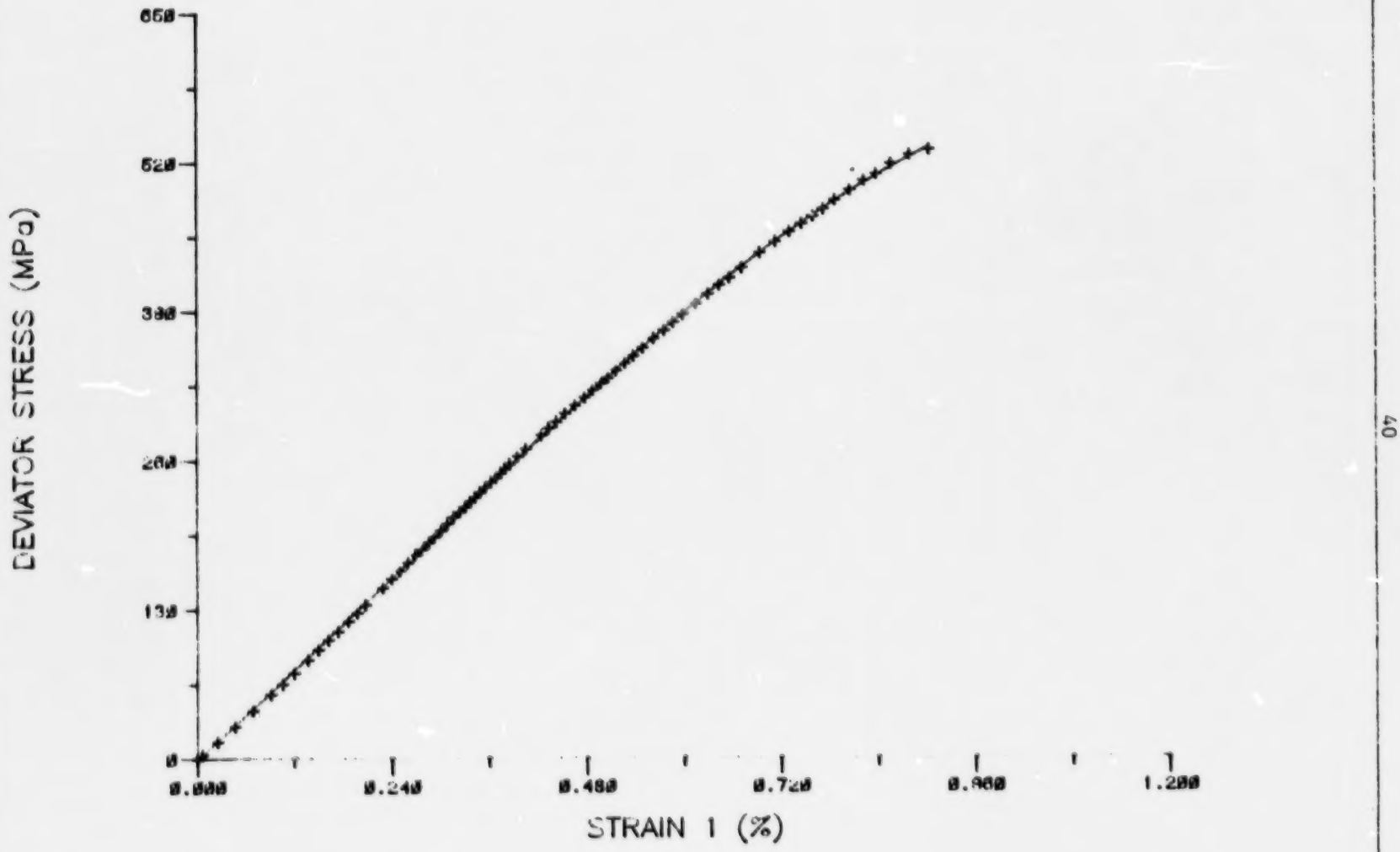

FIG. 25: DEVIATORIAL STRESS VS STRAIN: URL2 1080.93 (50.0 MPa)

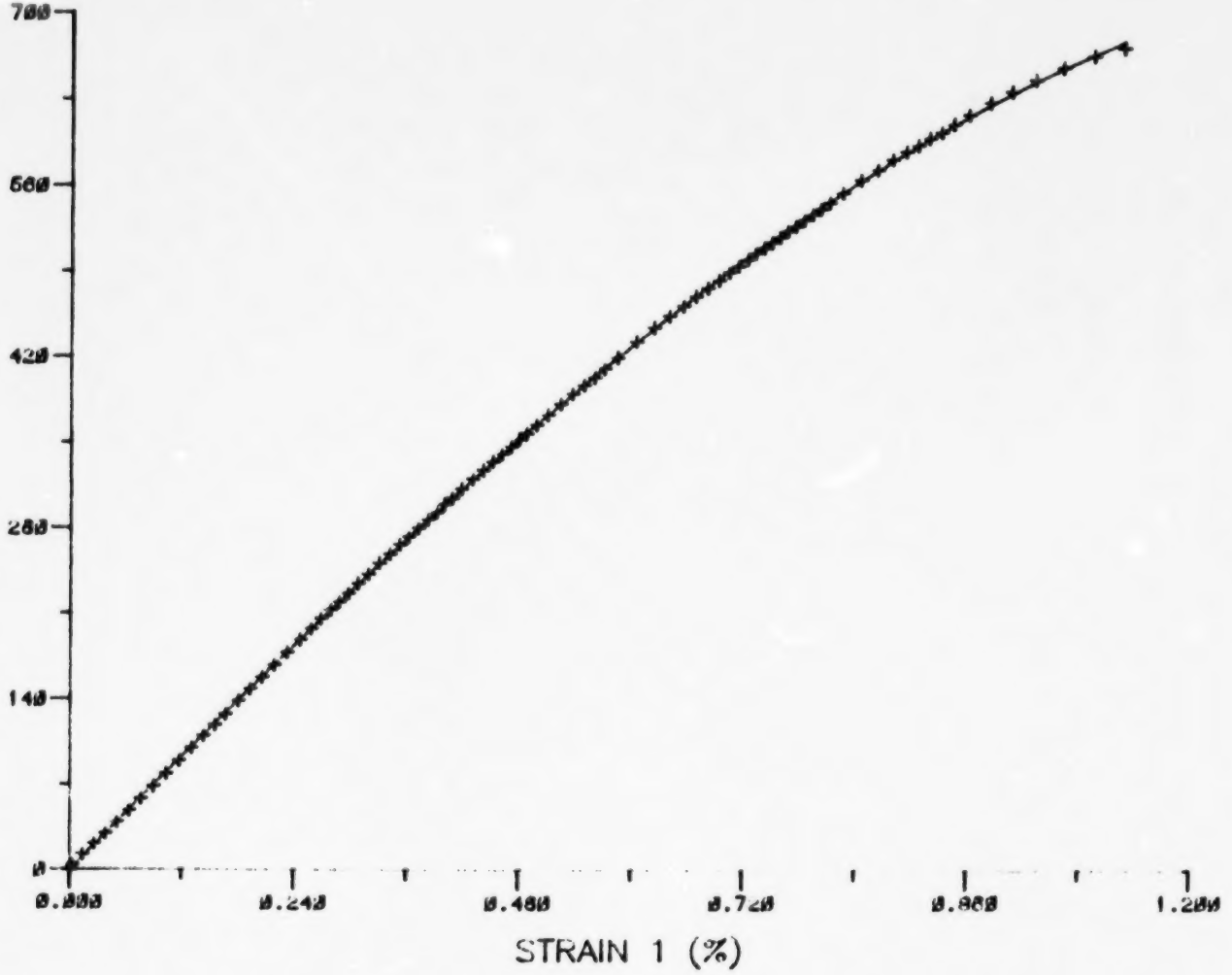

FIG. 26: DEVIATORIAL STRESS VS STRAIN: URL2 1082.31 (50.0 MPa)

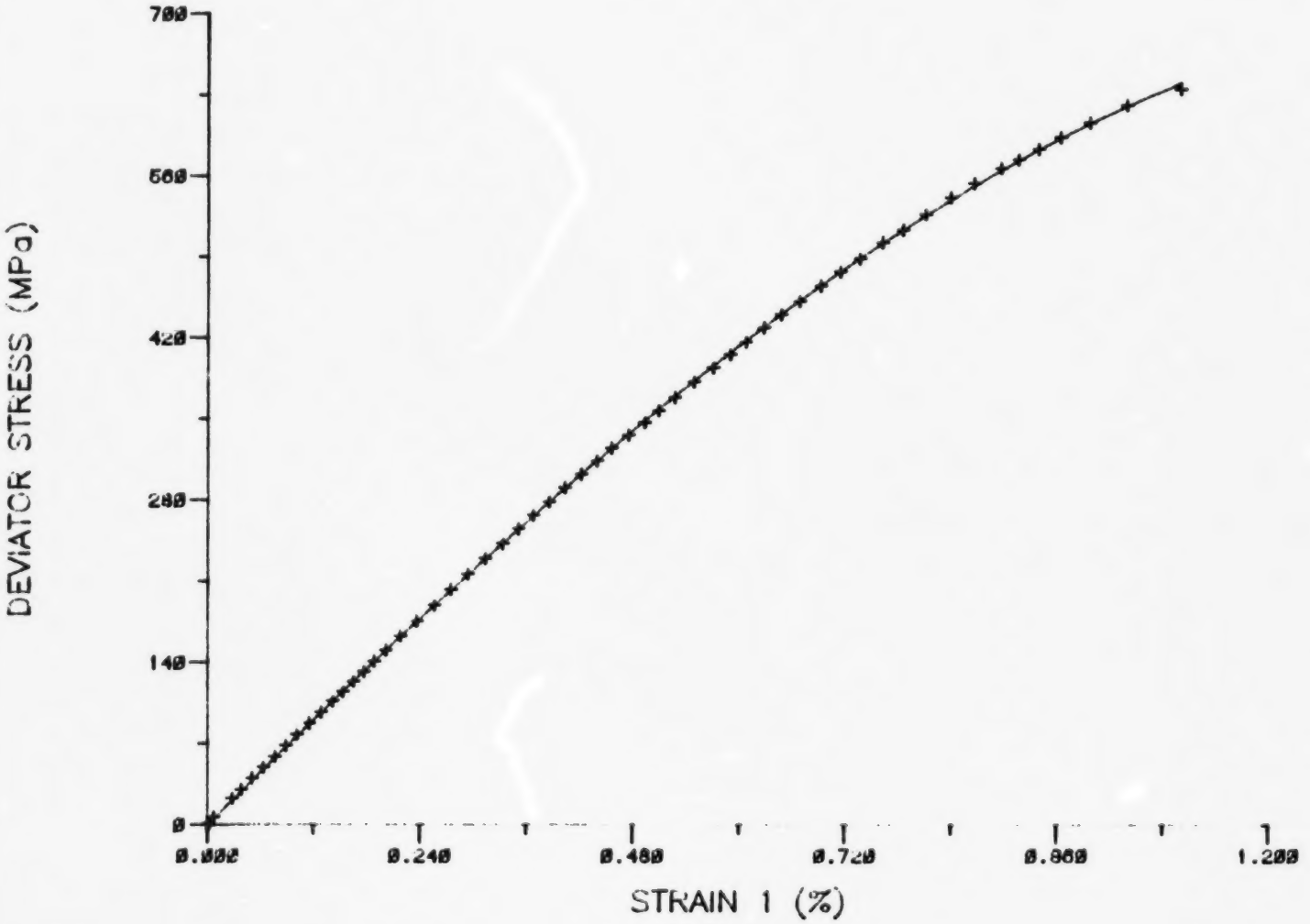

FIG. 27: DEVIATORIAL STRESS VS STRAIN: URL2 1080.63 (70.0 MPa)

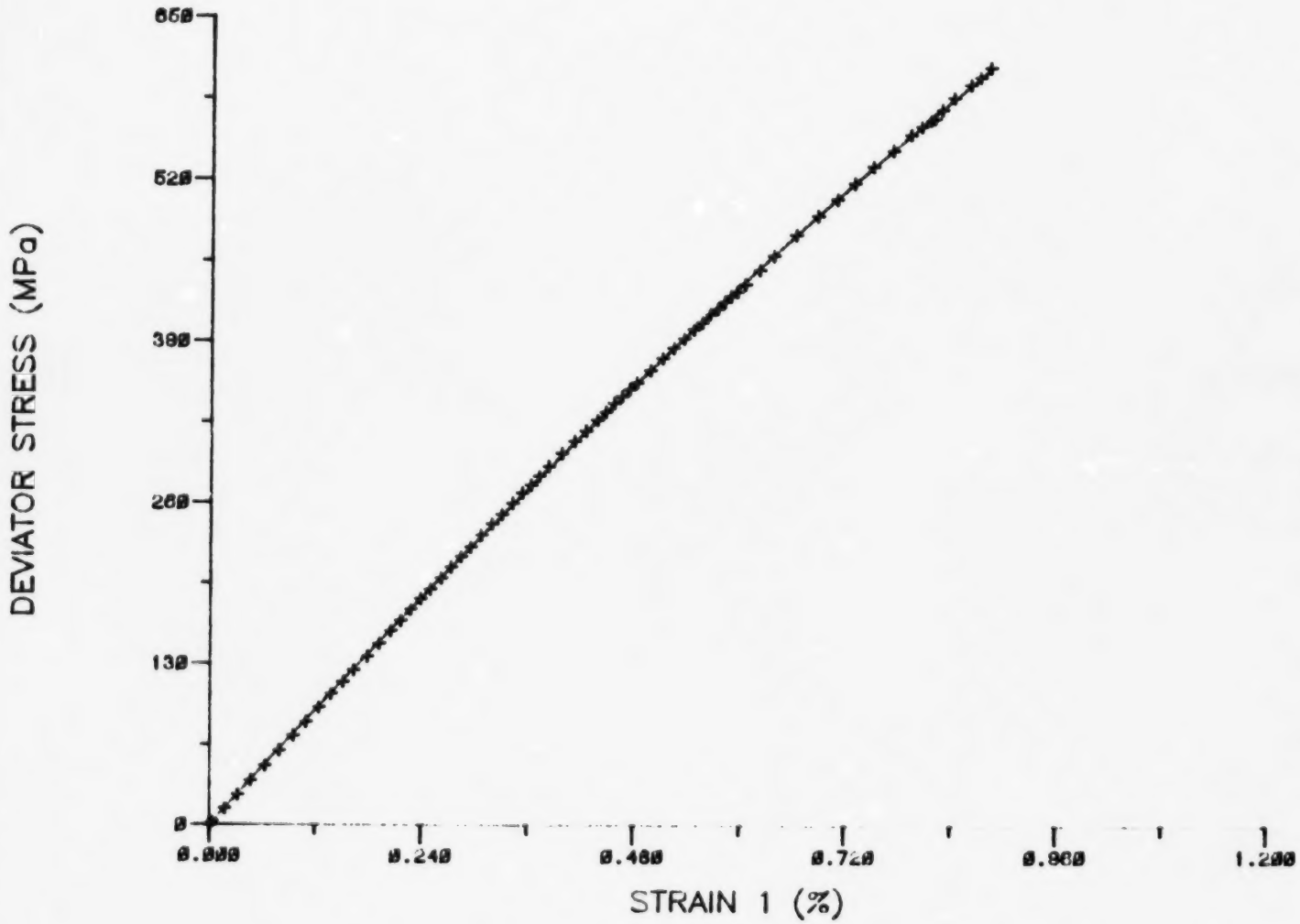

FIG. 28: DEVIATORIAL STRESS VS STRAIN: URL2 1082.03 (70.0 MPa)

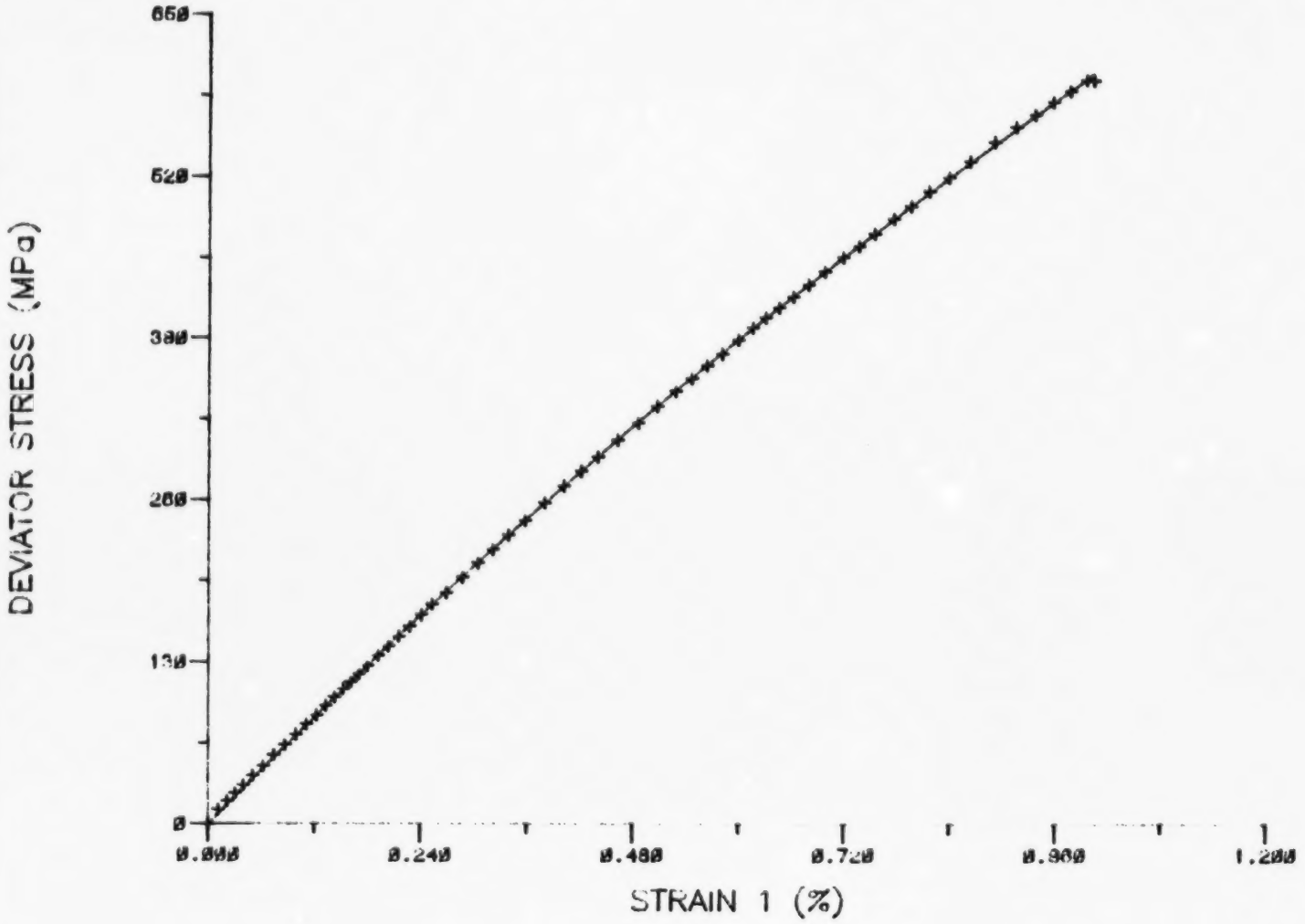

FIG. 29: DEVIATORIAL STRESS VS STRAIN: URL5 442.13 (15.0 MPa)

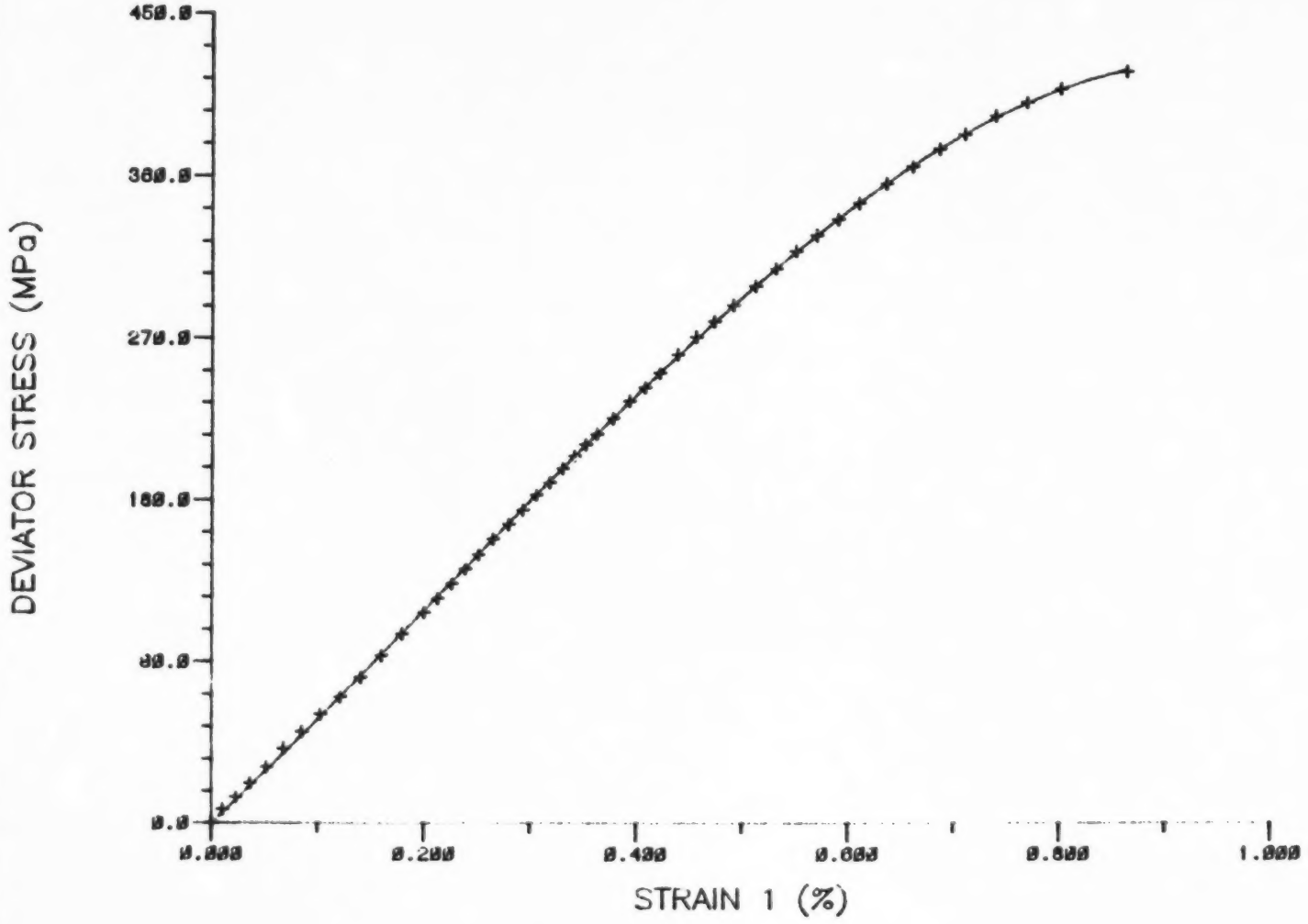

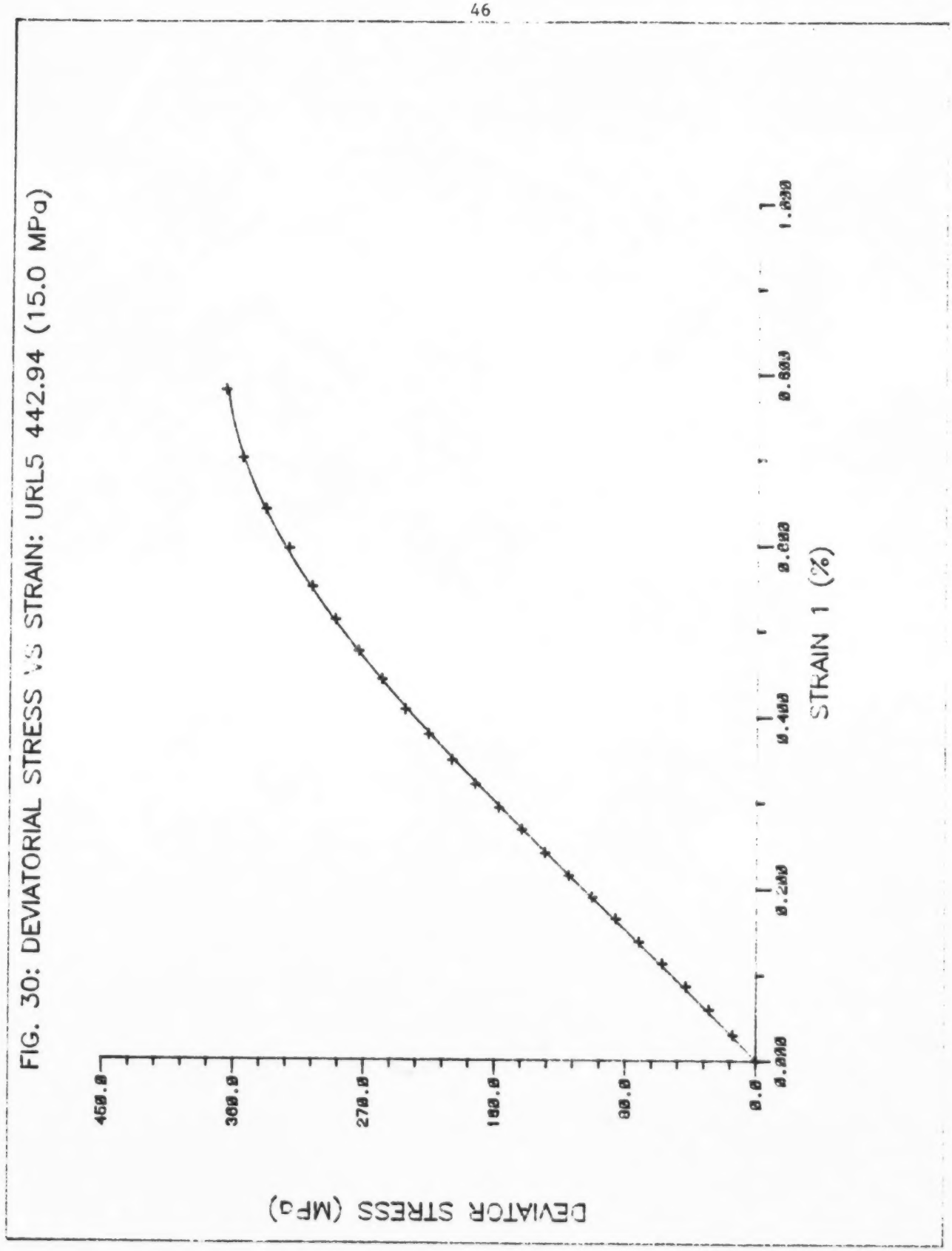

FIG. 30: DEVIATORIAL STRESS VS STRAIN: URL5 442.94 (15.0 MPa)

FIG. 31: DEVIATORIAL STRESS VS STRAIN: URL5 441.85 (30.0 MPa)

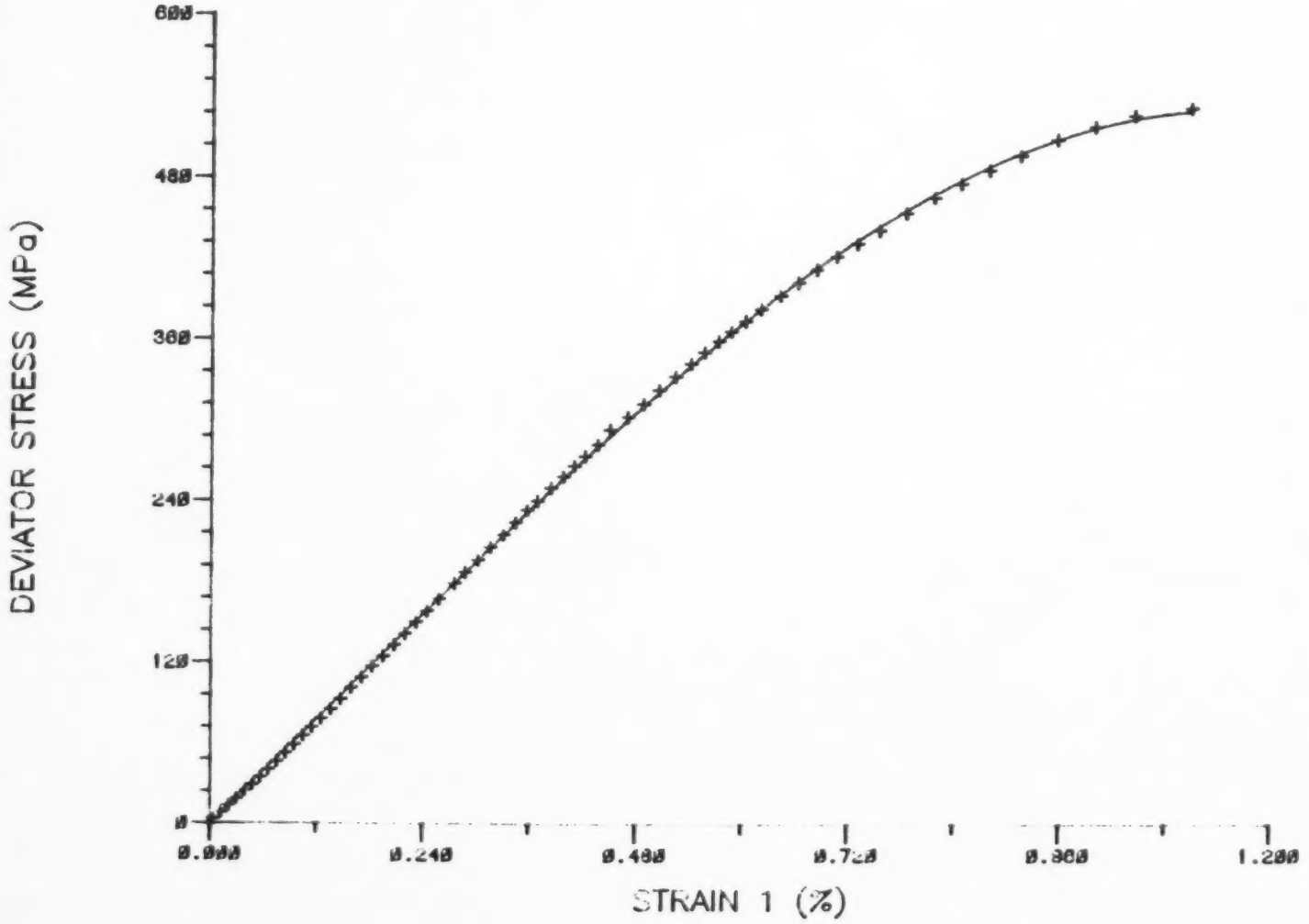

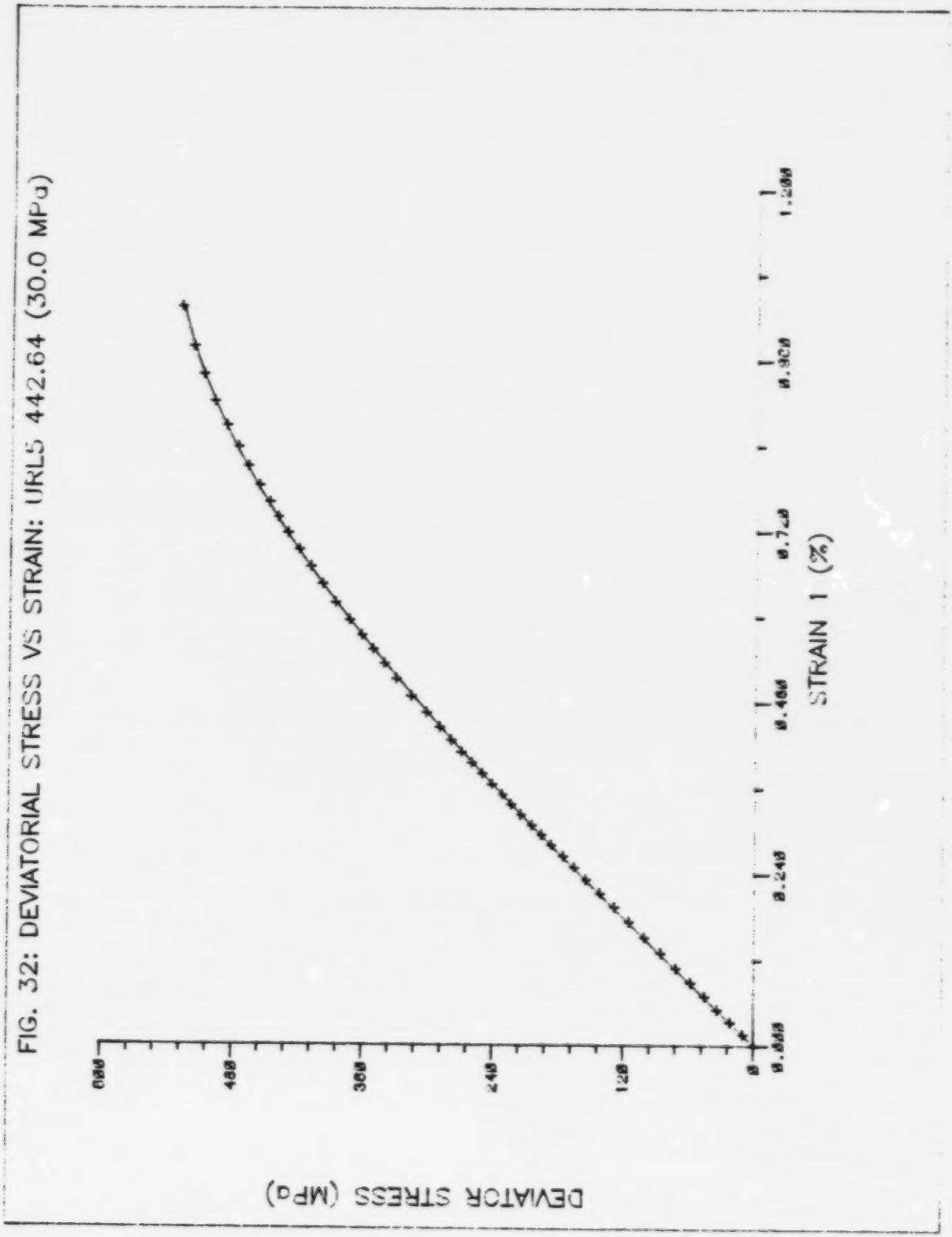

FIG. 32: DEVIATORIAL STRESS VS STRAIN: URLS 442.64 (30.0 MPa)

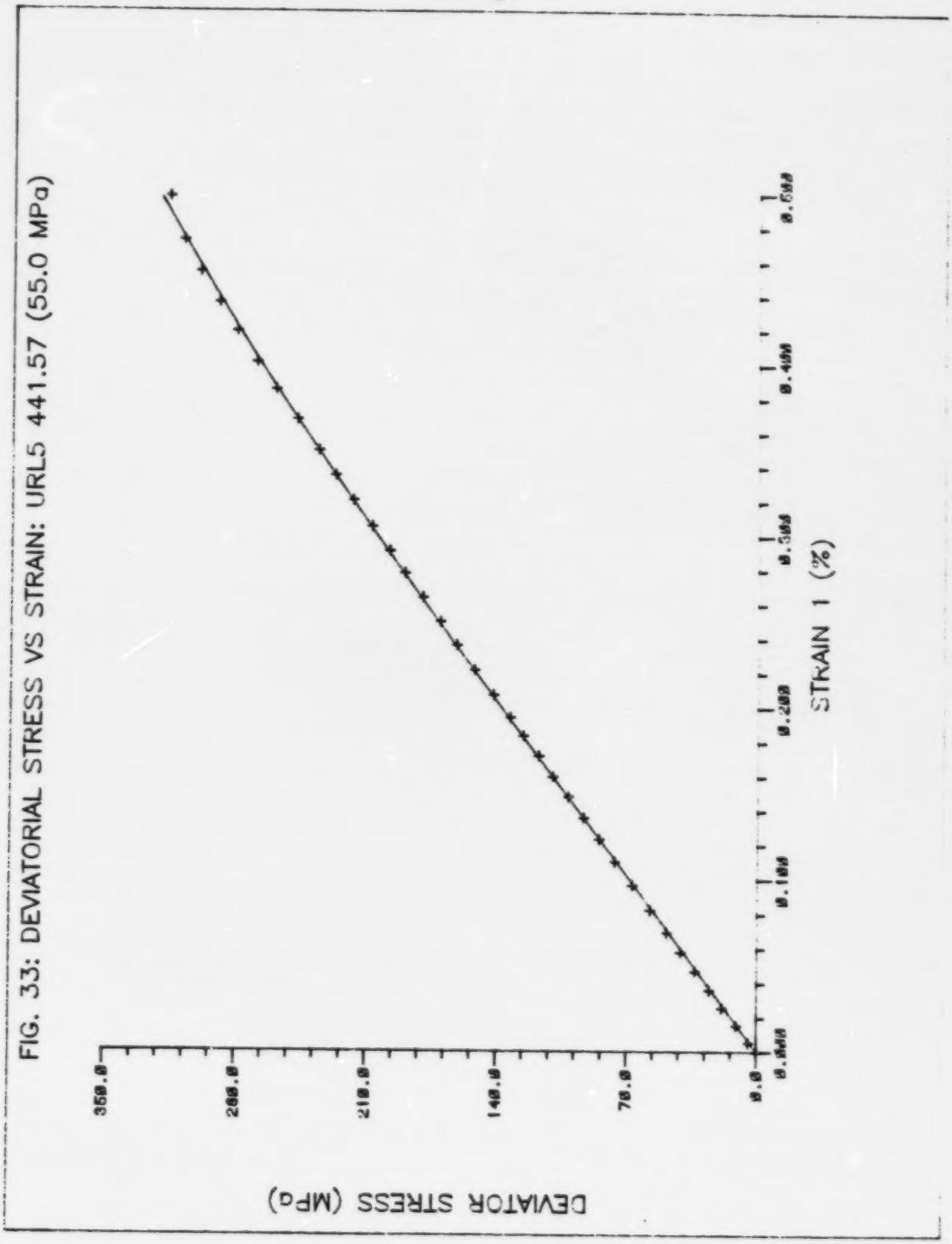

FIG. 33: DEVIATORIAL STRESS VS STRAIN: URL5 441.57 (55.0 MPa)

FIG. 34.: DEVIATORIAL STRESS VS STRAIN: URL5 442.36 (55.0 MPa)

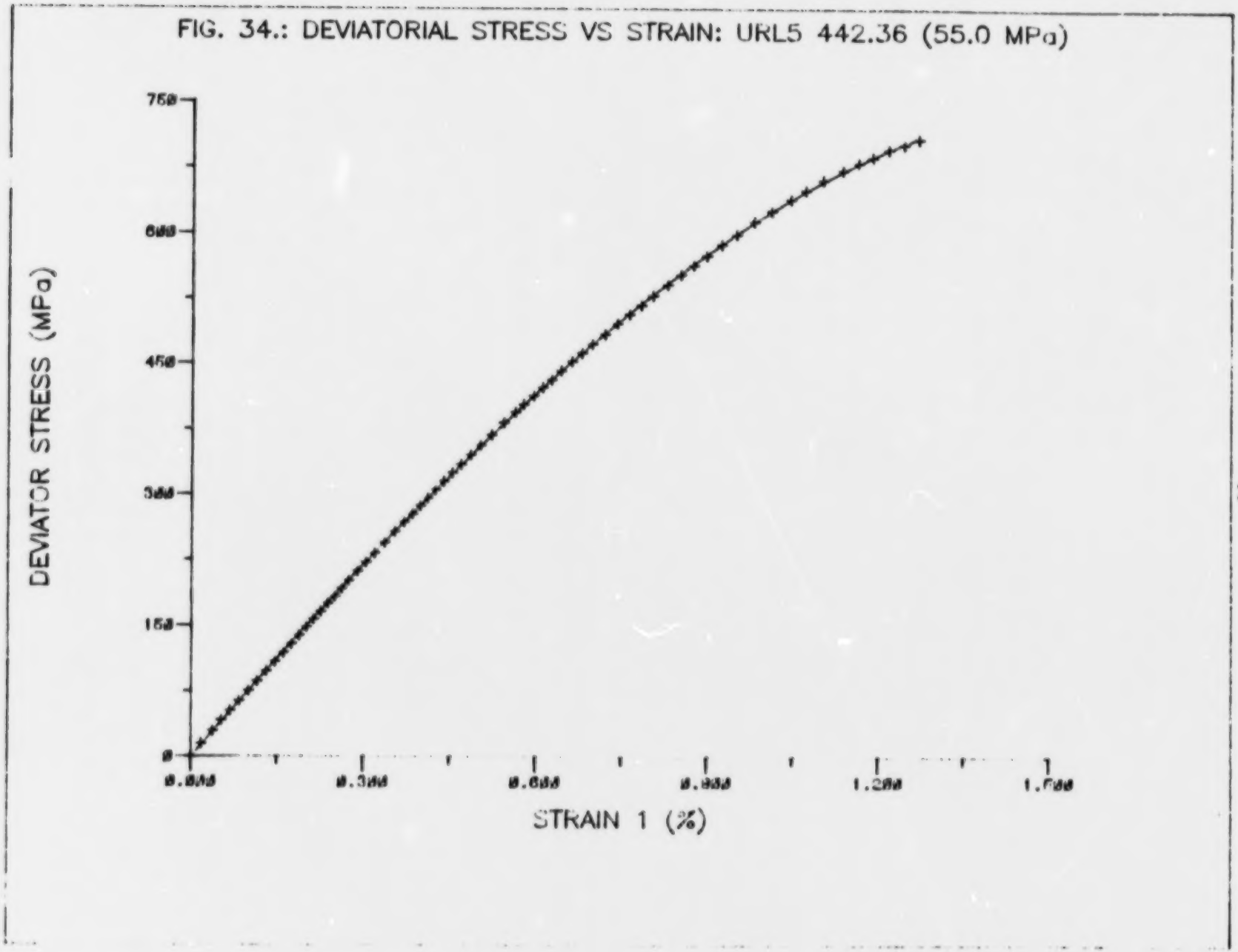

FIG. 35: DEVIATORIAL STRESS VS STRAIN: URL6 374.22 (5.0 MPa)

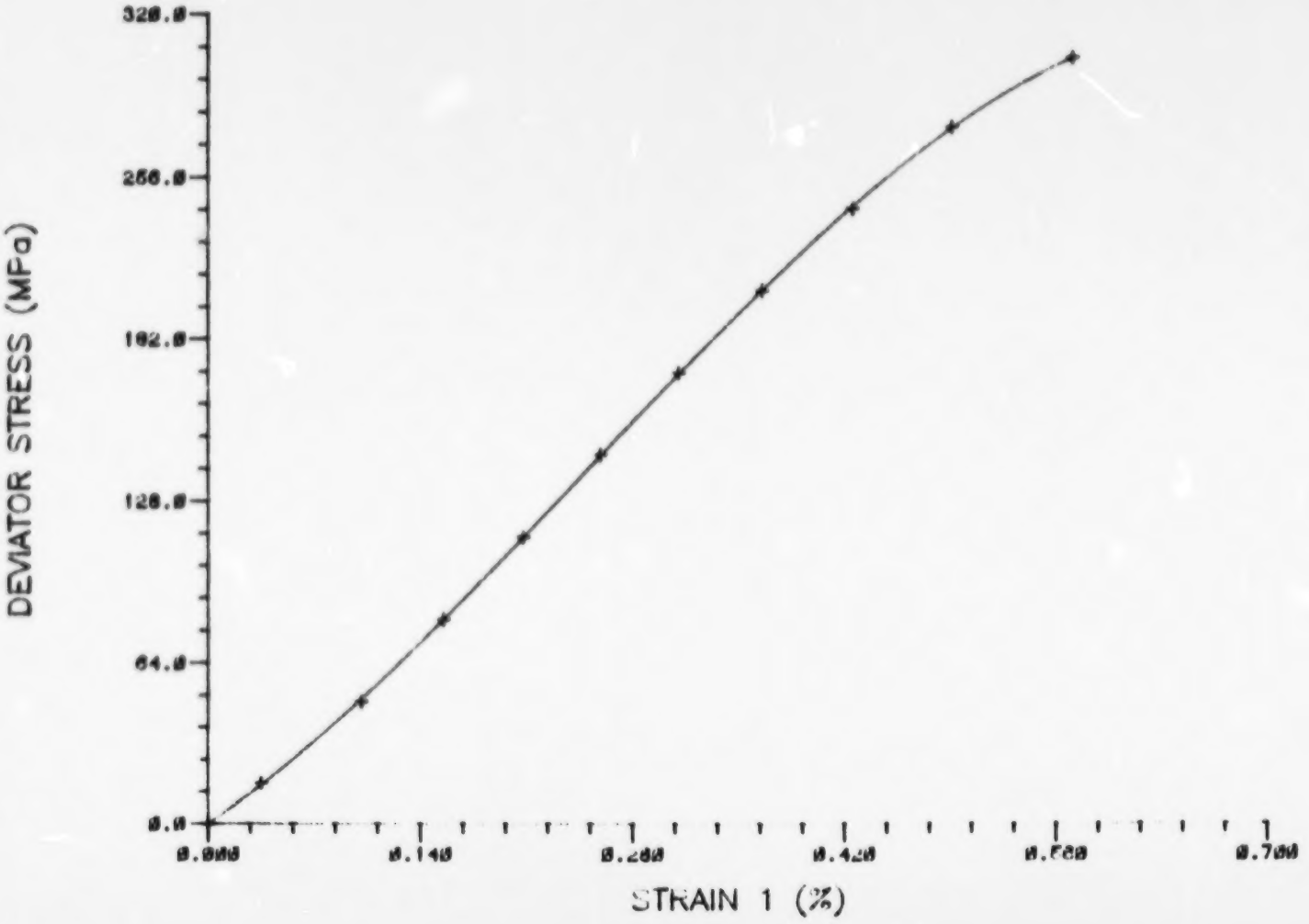

FIG. 36: DEVIATORIAL STRESS VS STRAIN: URL6 392.04 (5.0 MPa)

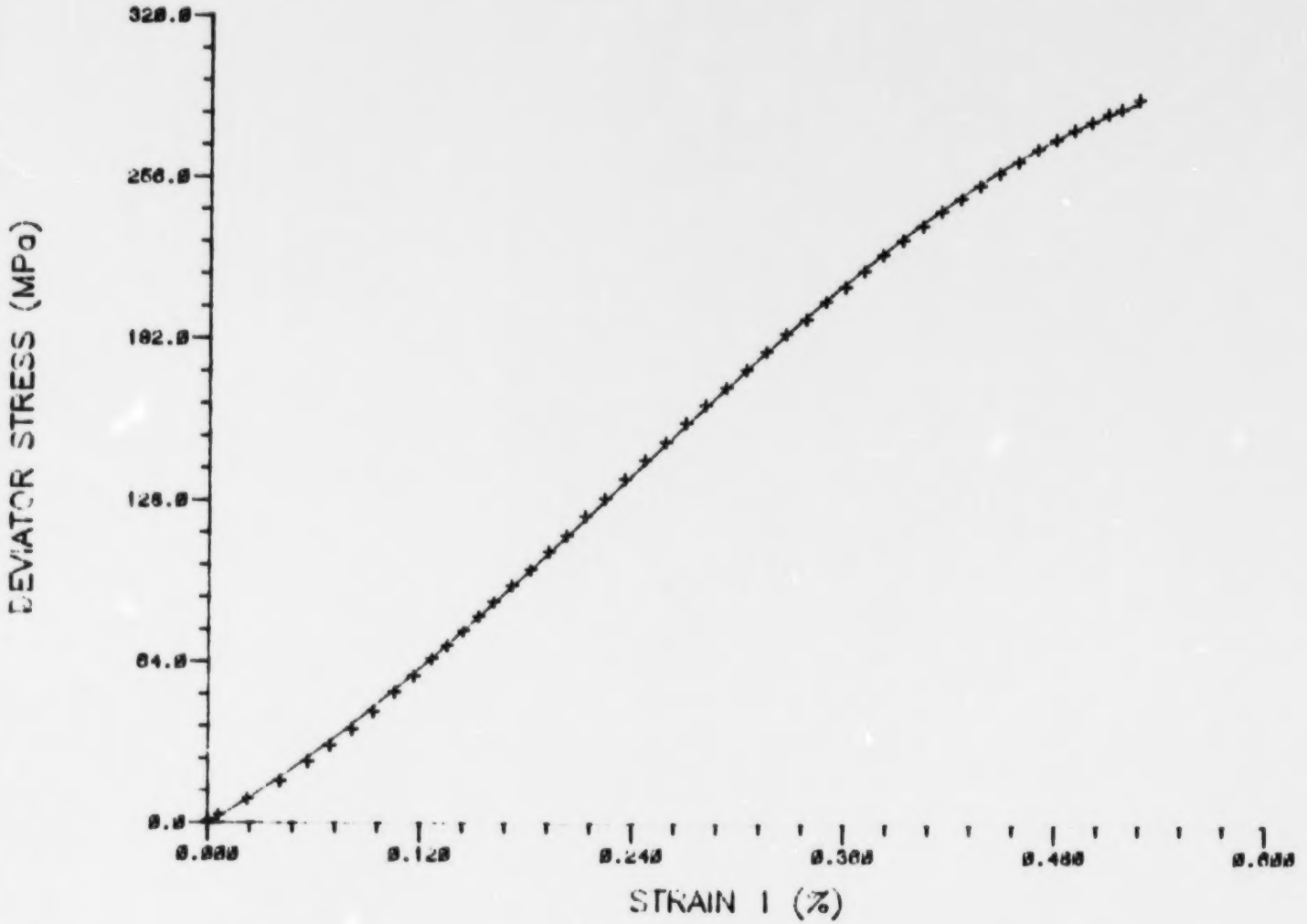

FIG. 37: DEVIATORIAL STRESS VS STRAIN: URL6 373.69 (10.0 MPa)

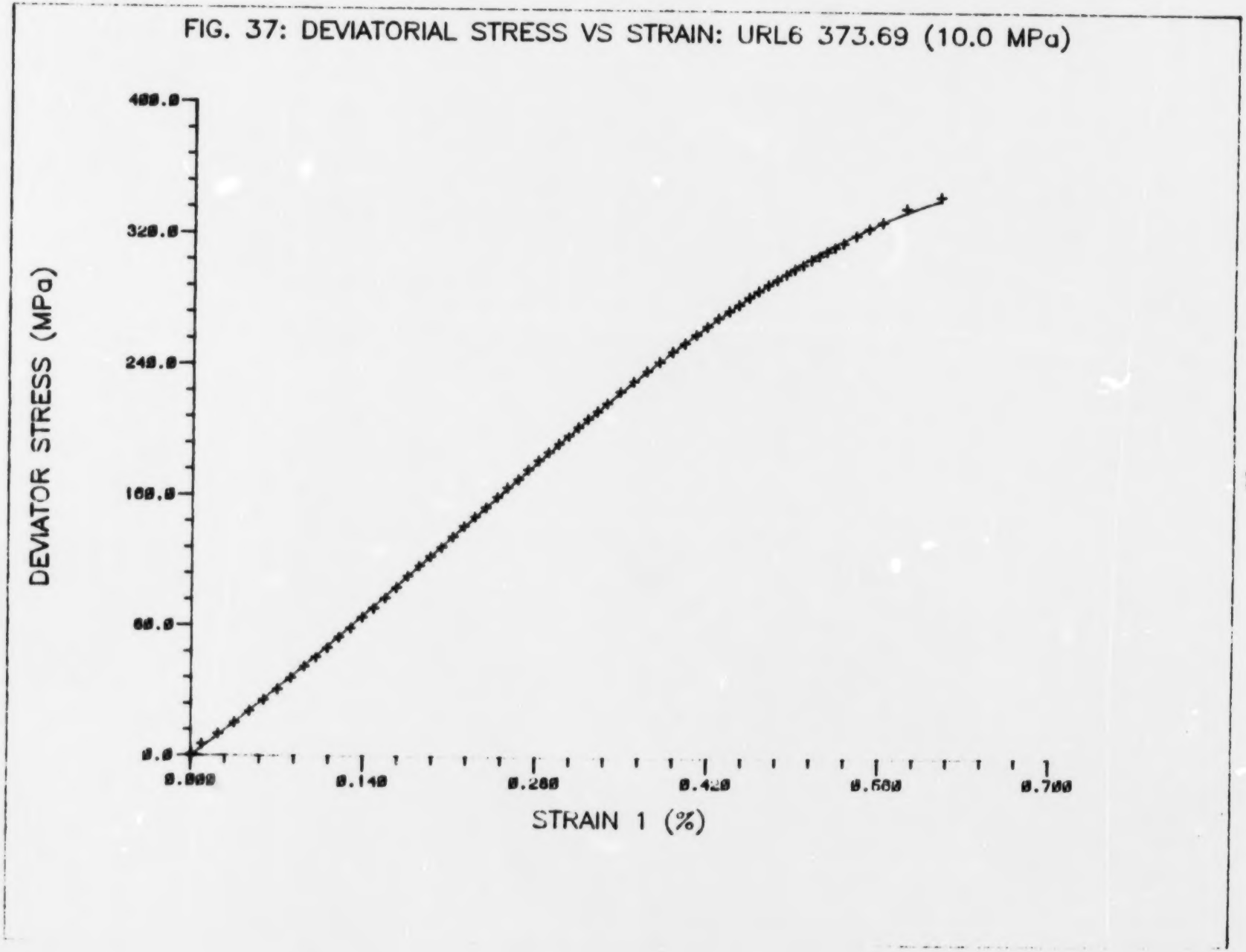

FIG. 38: DEVIATORIAL STRESS VS STRAIN: URL6 391.25 (10.0 MPa)

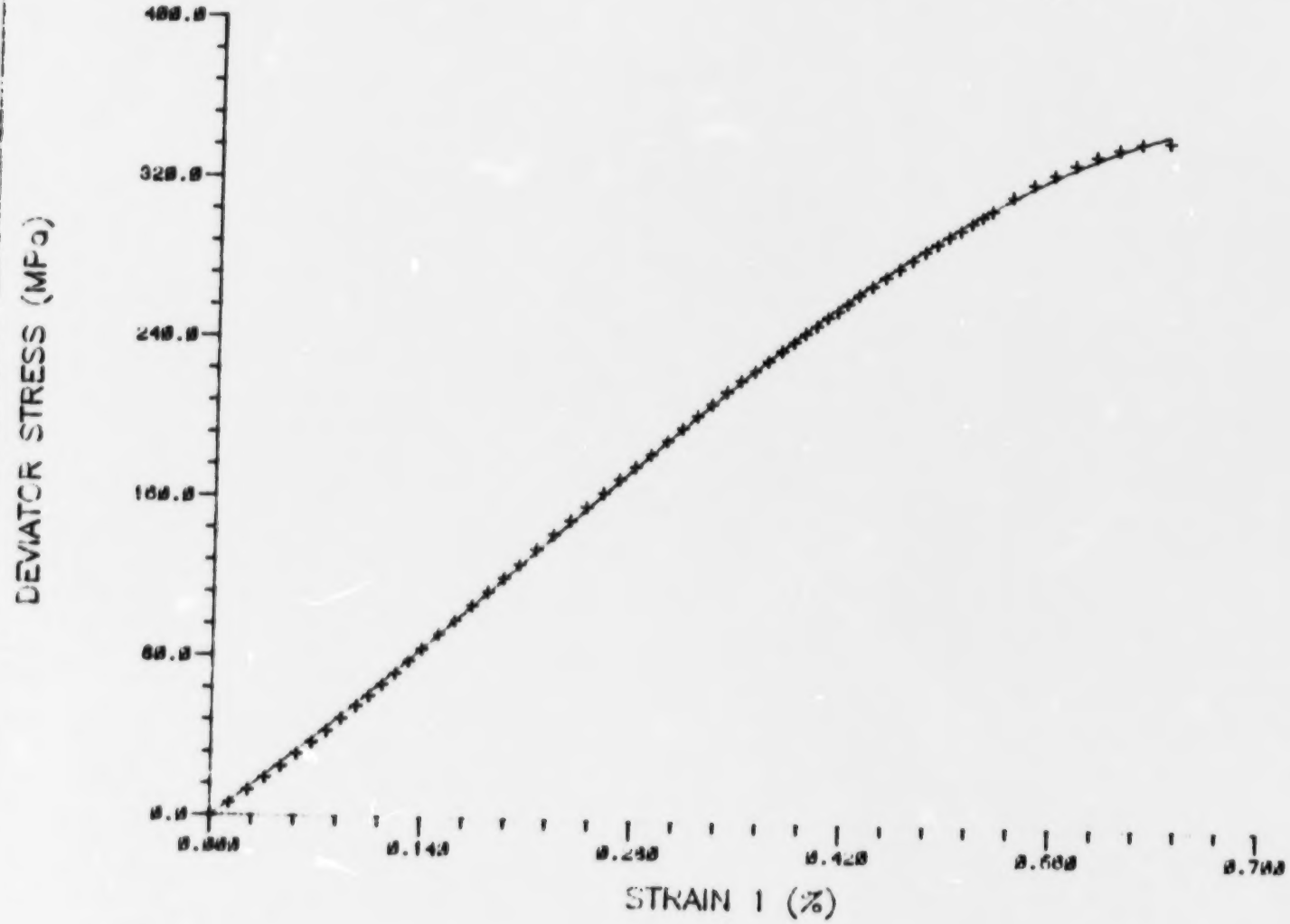

FIG. 39: DEVIATORIAL STRESS VS STRAIN: URL6 391.48 (25.0 MPa)

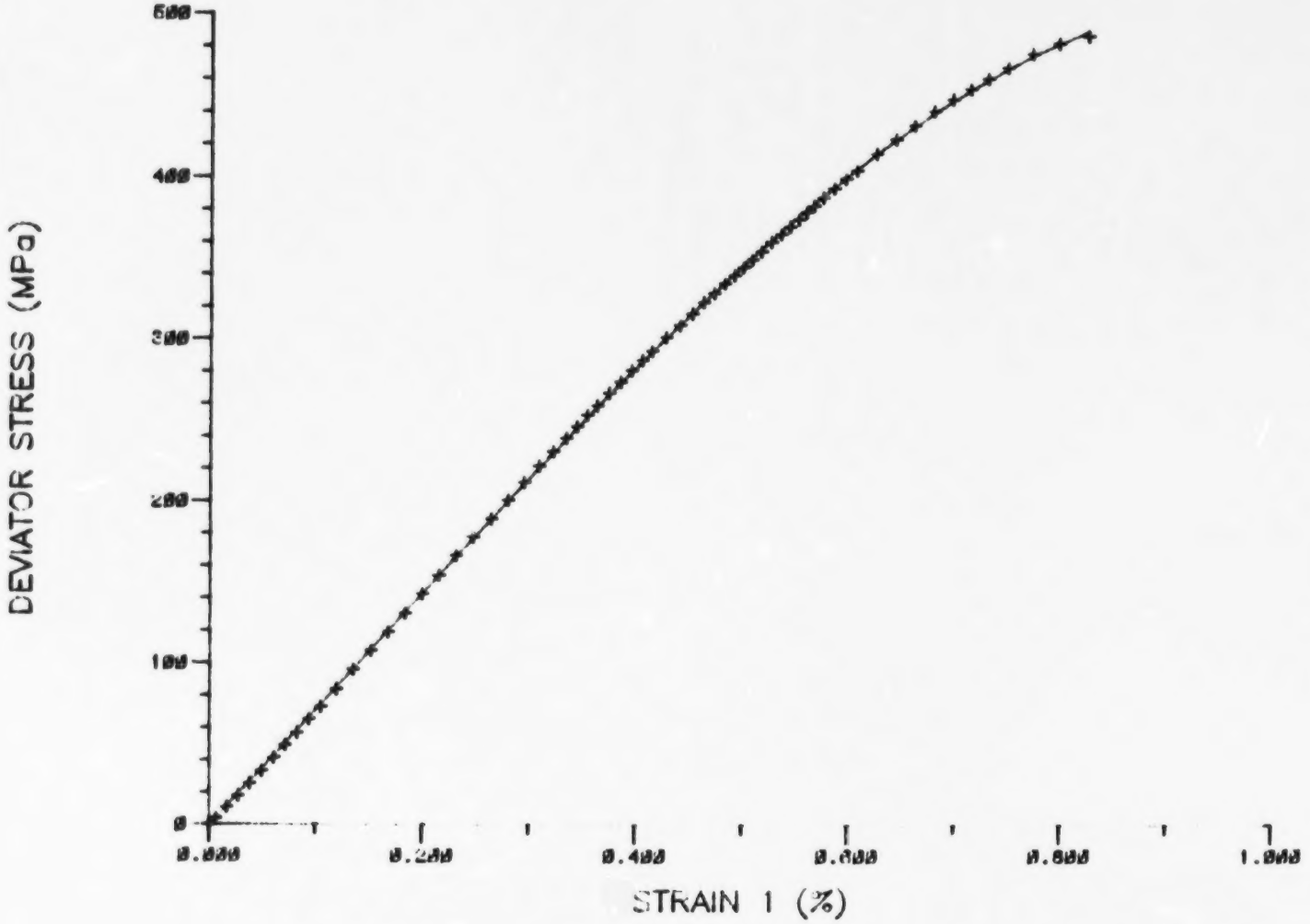

FIG. 40: DEVIATORIAL STRESS VS STRAIN: URL6 391.71 (25.0 MPa)

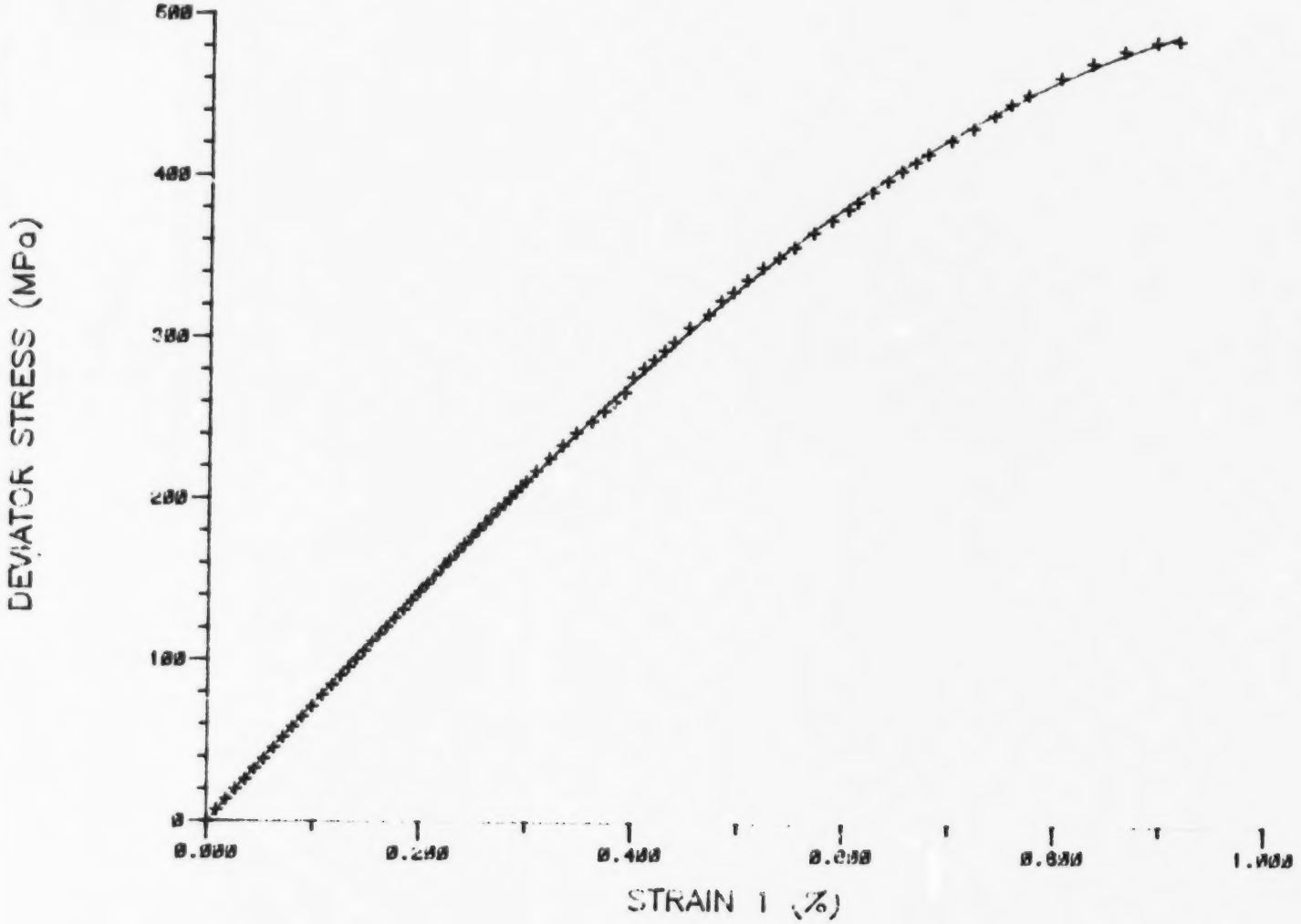

FIG. 41: DEVIATORIAL STRESS VS STRAIN: URL6 374.85 (50.0 MPa)

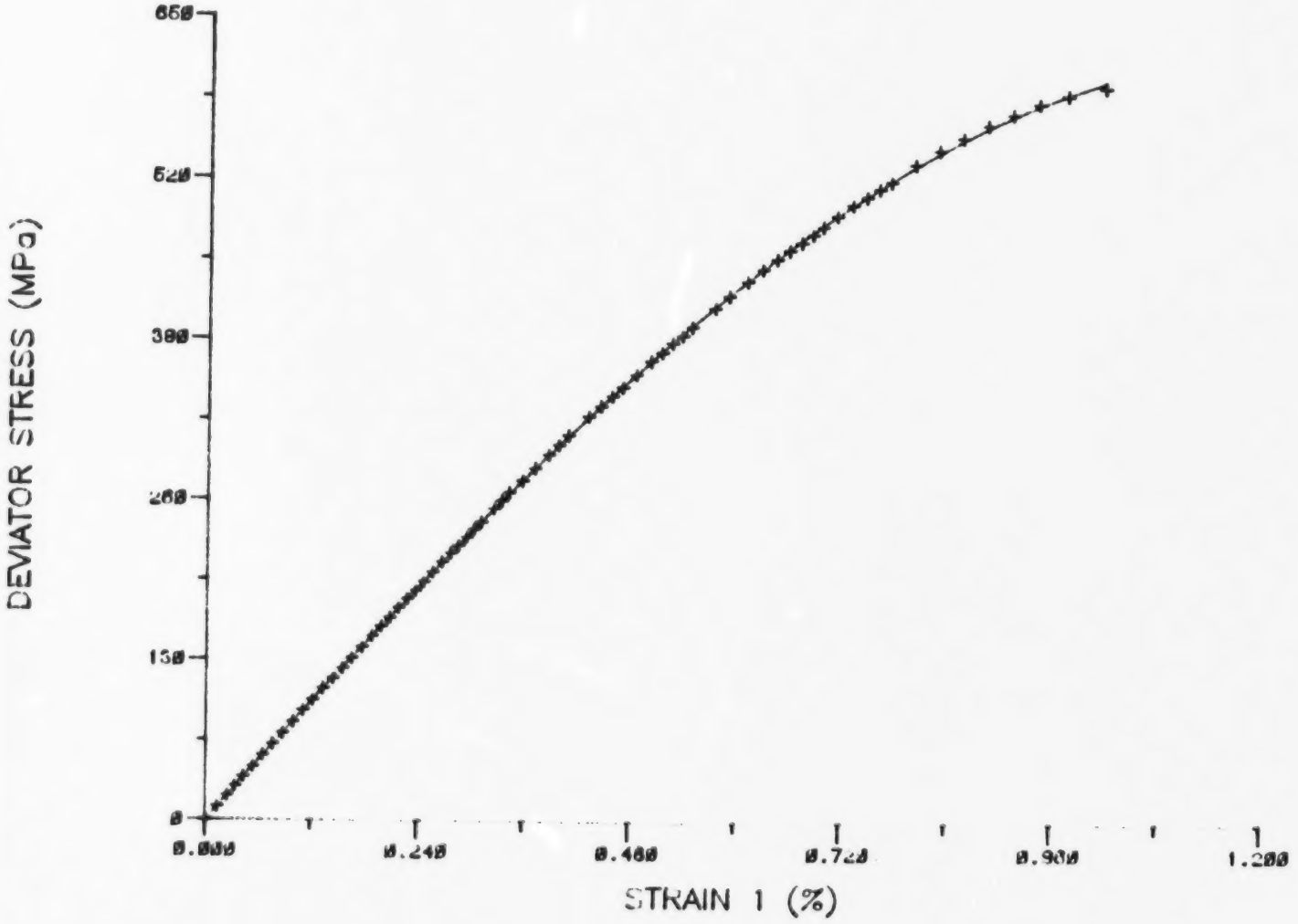

FIG. 42: DEVIATORIAL STRESS VS STRAIN: URL6 392.27 (50.0 MPa)